2006

Estimating the impact of 21st century climate change on wildfire risk potential

Meghna Tare
San Jose State University

ESTIMATING THE IMPACT OF 21st CENTURY CLIMATE CHANGE ON WILDFIRE RISK POTENTIAL

A Thesis

Presented to

The Faculty of the Department of Environment Studies

San Jose State University

In Partial Fulfillment

Of the Requirement for the Degree

Master of Science

By

Meghna Tare

May 2006

APPROVED FOR THE DEPARTMENT OF ENVIRONMENTAL STUDIES

Chair, Dr. Rachel O'Malley
Assistant Professor, Department of Environmental Studies,
San Jose State University

Dr. Stephen H. Schneider
Professor, Department of Biological Sciences
Co-Director, Center for Environmental Science and Policy
And Interdisciplinary Program in Environment and
Resources, Stanford University

Dr. Eugene Cordero, Assistant Professor, Department of
Meteorology, San Jose State University

Dr. Nathan L. Stephenson, Research Ecologist, USGS
Sequoia and Kings Canyon Field Station

APPROVED FOR THE UNIVERSITY

ABSTRACT

ESTIMATING THE IMPACT OF 21st CENTURY CLIMATE CHANGE ON WILDFIRE RISK POTENTIAL

by Meghna Tare

Fire occurrence in forests is driven by levels of fuel moisture content and, as such, is highly sensitive to changes in climate. Under current climate change projections, wildfire risk potential can be expected to increase significantly. Increased evaporation due to the increase in temperatures, will lead to more severe and longer-lasting droughts in some areas. Drought is an important indicator of fire in that it affects the amount of available fuel. Because of their low moisture content fuel becomes available during periods of drought, resulting in more intense fire. When studying the role of climate on the area of forest burned, several meteorological parameters like temperature, precipitation, and drought indexes such as the Keetch-Byram Drought Index (KBDI) have been used to study the relationship between climate and area burned by forest fires. This study will provide useful insights into the interconnections between 21st century climate change, drought, and forest fire for Sierra Nevada forests like Sequoia and Kings Canyon National Park based on the Keetch/Byram Drought Index. We explore this wildfire risk potential based on the highest and lowest intergovernmental Panel on Climate Change emission pathways. The results indicate more days exceeding "drought conditions," and a contrast between higher and lower emissions scenarios. It is important to understand and predict the potential of large fires to track the large-scale build up of forest fuels, and to develop warning systems and mitigation measures to protect and conserve the forest ecosystem. If climate change increases the future wildfire risk potential, we can expect changes in the behavior and response of plant and animal species, loss of habitat, and range shifts. Understanding ecosystem responses to climate change can help in predicting the ecological consequences of current and future climate change, in order to plan conservation strategies for warmer climates.

ACKNOWLEDGEMENT

"Real success is finding your lifework in the work that you love"…….

I absolutely enjoyed my research and writing this thesis, during which I have been supported and encouraged by many people. It was a very rewarding journey and now I have the opportunity to express my gratitude to them.

I am deeply indebted to my research advisor, Prof. Dr. Stephen Schneider of the Department of Biological Studies, and the Center for Environmental Science and Policy at Stanford University. He is not only a great scientist, who is a world authority on climate change, but a very encouraging person, with a great sense of humor. I feel honored to have him as my advisor and hope that I collected a few drops of his wisdom on my way towards this research work. I am also deeply indebted and thankful to my thesis committee members: Prof. Rachel O'Malley (SJSU), Prof. Eugene Cordero (SJSU), and Dr. Nathan Stephenson (USGS) for their valuable suggestions and ideas through out the course of this research.

As always it is impossible to mention everybody who contributed to this research work. My special thanks to: Edwin Maurer (Santa Clara University), Mike Mastrandrea (Stanford University), Pasha Groisman (NOAA), Amy Luers (Union of Concerned Scientists), Tony Caprio (USGS), Prof. Thomas Swetnam (University of Arizona), Anthony Westerling (Scripps Institute of Oceanography), Tom Okey and Bruce Wright (Conservation Science Institute). Many more people and friends participated in various ways to ensure my research succeeded and I am thankful to them all. And lastly, I would like to thank my husband, Sandeep. He has been a constant source of inspiration and creative criticism. He is a computer engineer, but now he knows as much about climate change and forest fires as I do.

TABLE OF CONTENTS

LIST OF FIGURES

LIST OF TABLES

INTRODUCTION AND BACKGROUND

What is Climate Change and Global Warming?

Climate change refers to the variation in the Earth's global climate or regional climates over time. It describes changes in the variability or average state of the atmosphere - or average weather - over time scales ranging from decades to millions of years. These changes may come from internal processes, be driven by external forces or, most recently, be caused by human activities. In recent usage, especially in the context of environmental policy, the term "climate change" is often used to refer to the ongoing changes in modern climate, including the average rise in surface temperature known as global warming.

Global warming is a phrase that refers to the effect of human activities on the climate, in particular through the burning of the fossil fuels (coal, oil, and gas) and large-scale deforestation-activities. These activities have increased enormously since the industrial revolution, and are currently leading to the release of about 7 billion tones of carbon as carbon dioxide into the atmosphere each year together with substantial quantities of methane, nitrous oxide and chlorofluorocarbons (CFC's). These gases are known as greenhouse gases. Such gases absorb infrared radiation emitted by the Earth's surface and act as blankets over the surface keeping it warmer that it would otherwise be. The greenhouse effect of our atmosphere increases the surface temperatures to $+15^{0}$C and helps in sustaining life on earth. It is known as the greenhouse effect because the glass in a greenhouse possesses similar properties to the greenhouse gases in that it absorbs infrared radiation while being transparent to radiation in the visible part of the spectrum (Figure 1). The degree of the greenhouse effect is dependent primarily on the concentration of these greenhouse gases. Because of our industrial and agricultural activities, we are in the process of increasing the concentration of these greenhouse gases, which adds to the "blanket" of heat-trapping gases in the atmosphere, altering the radiation balance and further increasing surface temperatures.

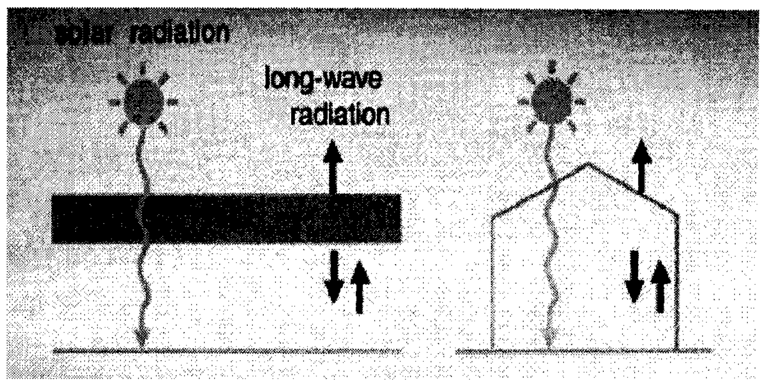

Figure 1: The greenhouse effect

Reprinted: Houghton, J. 2005. Global warming. *Rep. Prog. Phys.* 68:1343–1403.

Global Warming Trends and Projections

The scientific opinion on climate change, as expressed by the UN Intergovernmental Panel on Climate Change (IPCC) and explicitly endorsed by the national science academies of the G8 nations, is that the average global temperature has risen 0.6 ± 0.2 °C since the late 19th century, and that it is likely that "most of the warming observed over the last 50 years is attributable to human activities." About two-thirds of this warming took place between 1900 and 1940. Global temperatures declined slightly from the 1940s through the 1970s; but have risen more rapidly during the last 25 years than in the period before 1940 (Figure 2).

Atmospheric carbon dioxide has increased from around 280 parts per million (by volume) in 1800 to around 315 in 1958 and 367 in 2000, a 31% increase over 200 years. Other greenhouse gas emissions have also increased. Future carbon dioxide levels are expected to continue to rise due to ongoing fossil fuel usage, though the actual trajectory will depend on uncertain economic, sociological, technological, and natural developments. The Intergovernmental Panel on Climate Change has concluded that there will be both global and regional climatic change, altered precipitation patterns, occurrence of extreme events, particularly related to temperature and precipitation, and an increase in climate variability (Houghton et al., 2001) during the next 100 years (IPCC, 1995, 2001).

The IPCC Special Report on Emissions Scenarios (SRES) projections shows that the atmospheric concentration of carbon dioxide will probably increase significantly during the next century (IPCC, 2001). According to the report, carbon dioxide emissions from the combustion of fossil fuels and from land-use changes (primarily tropical deforestation) are projected to range from about 5 to 35 GtC per year in the year 2100 compared to the average emissions during the 1990s of about 7.5 GtC per year. Such a range of emissions would mean that the atmospheric concentration of carbon dioxide would increase from today's level of about 375 ppm to between about 540 and 970 ppm by 2100. Global mean surface temperatures are projected to increase between 1990 and 2100 by about 1.4 to 5.8°C (IPCC, 2001). Warmer temperatures will cause an intensification of the hydrologic cycle, with increased evaporation over both land and water. The higher evaporation rates in turn will lead to greater drying of soils and vegetation, especially during the warm season.

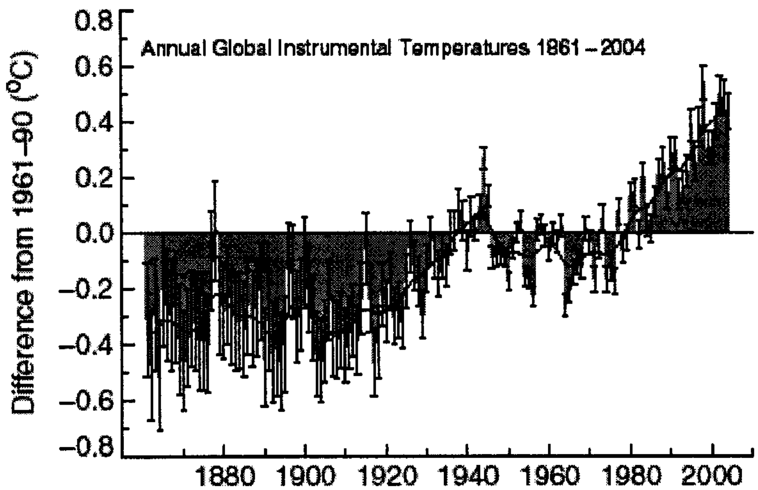

Figure 2: Global temperature changes (1880-2000)

Reprinted from: Houghton, J. 2005. Global warming. *Rep. Prog. Phys.* 68:1343–1403.

Potential Consequences of Global Warming

Warmer temperatures could increase the probability of drought. Greater evaporation, particularly during summer and fall, could exacerbate drought conditions and increase the risk of wildfires. For example, in 2002, the Western United States experienced its second worst wildfire season in the last 50 years; more than 7 million acres burned. Colorado, Arizona, and Oregon had their worst seasons (Swetnam, 2003). The globally averaged surface temperature is projected to increase by 1.4 to 5.8 ^{0}C during the next 100 years, depending on the climate models and development scenarios used. Increased heat waves due to climate change would cause more heat-related illness and death. These conditions could also aggravate local air quality problems.

Climate change affects the occurrence and spread of disease by impacting the population size and range of hosts and pathogens, the length of the transmission season, and the timing and intensity of outbreaks. In general, warmer temperatures and greater moisture will favor extensions of the geographical range and season for vector organisms such as insects, rodents, and snails. This in turn leads to an expansion of the zone of potential transmission for many vector-borne diseases, among them malaria, dengue fever, yellow fever, and some forms of viral encephalitis. Extreme weather events such as heavy rainfall or droughts often trigger disease outbreaks, especially in poorer regions where treatment and prevention measures may be inadequate. The geographic ranges of most plant and animal species are limited by climatic factors, including temperature, precipitation, soil moisture, humidity, and wind. Any shift in the magnitude or variability of these factors in a given location will impact the organisms living there. Species sensitive to temperature may respond to a warmer climate by moving to cooler locations at higher latitudes or elevations (McMichael et al, 1996).

Glaciers, coral reefs, atolls, mangroves, boreal and tropical forests, polar and alpine ecosystems, prairie wetlands, and remnant native grasslands can be especially vulnerable to climate change because of limited adaptive capacity. Some natural systems are at risk of significant and irreversible damage. While some species may increase in abundance or range, climate change will increase existing risks of extinction of already threatened or vulnerable species and biodiversity loss. In 1998 coral reefs around the world experienced the most extensive and severe bleaching in recorded history. If the overall warming is accompanied by more frequent periods of sustained high temperatures, mass bleaching events will become more frequent and widespread. Projected adverse impacts include reductions in crop yields in most tropical and sub-tropical regions; decreased water availability in many regions that already experience water scarcity; an increase in certain diseases, heat stress mortality and risk of flooding; and increased energy demand for cooling during warmer summers (Wilkinson et al., 1999).

The observed changes in response to 21st century warming include shrinking glaciers, thawing permafrost, earlier break-up of river and lake ice, lengthening of mid- to high-latitude growing seasons, pole-ward and altitudinal shifts of plant and animal ranges, declines of some animal and plant populations, and earlier tree flowering, insect emergence and egg-laying in birds; significant slowing of ocean circulation that transports warm water to the North Atlantic; large reductions in the Greenland and West Antarctic ice sheets; and releases of additional greenhouse gases from permafrost regions and coastal sediments.

Global warming may also have positive effects. Despite the limiting factor of water, an increase in carbon dioxide concentration has the direct effect of increasing the transpiration efficiency of most plants so that they actually produce more net biomass per unit of water used by the plant. In middle and higher latitudes, global warming will extend the length of the potential growing season, allowing earlier planting of crops in the spring, earlier maturation and harvesting, and the possibility of completing two or more cropping cycles during the same season. With global warming, soil degradation is more likely to occur, and soil fertility would probably be affected by global warming. However, due to the fact that the ratio of carbon to nitrogen is a constant, a doubling of carbon is likely to imply a higher storage of nitrogen in soils as nitrates, thus providing higher fertilizing elements for plants, providing better yields. In the long run, the climatic change could affect agriculture in several ways (Fischer, et al, 2002).

CLIMATE CHANGE AND FOREST FIRES

Certain conditions must be present for wildfires to occur. The most common conditions include: hot, dry and windy weather; the inability of fire protection forces to contain or suppress the fire; the occurrence of multiple fires that overwhelm committed resources; and a large fuel load (dense vegetation). Once a fire has started, several conditions influence its behavior, including fuel topography, precipitation amounts and timing weather, drought and development (Stephens et al. 2003). Increasing temperature alone does not necessarily guarantee greater fire extent (Flannigan et al., 2000; Fried et al., 2004). Weather patterns combined with certain geographic locations can create a favorable climate for wildfire activity. Areas where annual precipitation is less than 76 cms per year are extremely fire susceptible. Topography influences the movement of air, thereby directing a fire course. For example, if the inclination (measured as percentage) of uphill slope doubles, the rate of spread in wildfire will likely double. With periods of drought the fuel moisture drops significantly adding to increased fire danger. Where we expect low moisture content in the fuels during summer months, with drought conditions, the fuels reach these same low numbers earlier in the year, prolonging the high fire danger period.

The average annual area burned reported for the western US increased dramatically in the last three decades (Brown et al., 2004). Large wet areas promote more fuel loading, and large dry areas decrease fuel moisture and thus increase the fire risk in both the cases. In the forested areas where heavy fuels tend to accumulate over long periods, such as in the Northwest and at higher elevations around the west, anomalously dry conditions have a greater effect on fire danger (Swetnam, 1998; Brown, 2004). Warmer climate may cause more frequent and more severe fires in the western United States (Lenihan et al., 1998; Mckenzie et al., 2004). Global circulation models also suggests that the length of the fire season, as expressed by measures such as temperature, drought indices, degree-days, and fire weather indices, will likely be longer, suggesting that we can expect more fires to occur during a given year (McKenzie et al., 2004).

Fire Regime

A fire regime is a generalized description of the role fire plays in an ecosystem, and has six components: fire frequency, size, intensity, seasonality, type and severity. Fire frequency affects ecosystems through interrupting, terminating or facilitating individuals' life cycles. Fire size determines landscape patchiness and determines the distance seeds will have to travel for regeneration. Fire intensity is the amount of energy released (per unit time and burning fire front) during a fire, and within the confines of a single burn, can vary greatly depending on fuel type and loading, topography, and meteorological influences. The season of the year in which fire occurs is one the determinants of the successional trajectories on which ecosystems embark after fire. Fire type refers to crown, surface and ground fires, which are largely controlled by fire intensity and fuel characteristics. Fire severity is a measure of ecosystem effects. The fire regime at any location will probably change over time due to these interactions between weather and forest fuel. If future climate change results in an altered fire regime will that new fire regime precede or follow a change in vegetation? Describing the variability of climate and its influence on fire regimes is critical for establishing reference conditions as targets for forest management.

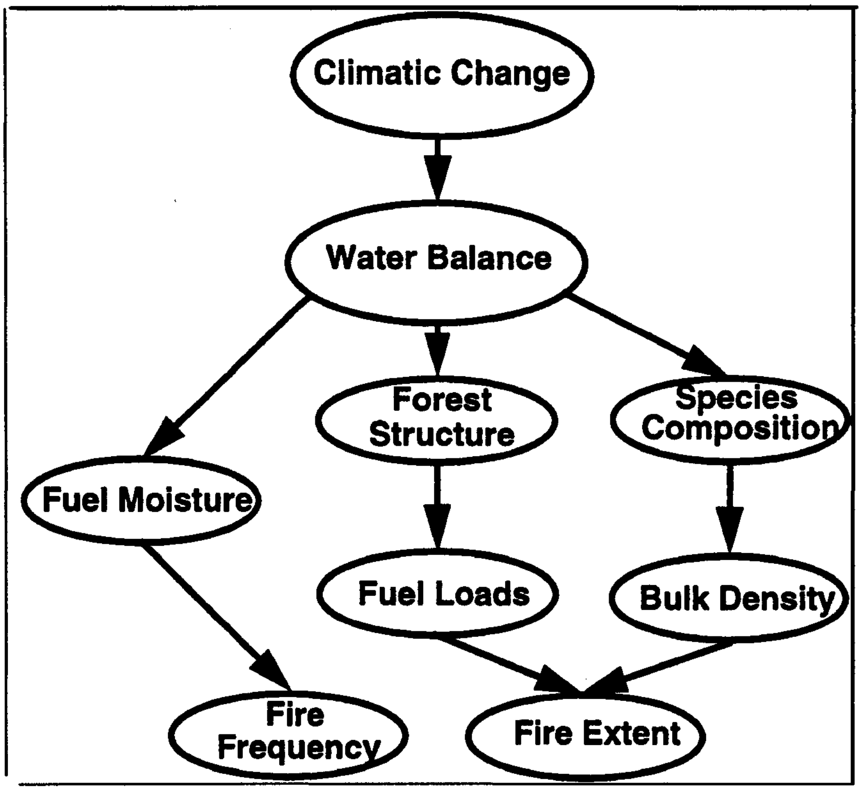

Figure 3: Major direct and indirect interactions among climate, forest structure, species composition, and the fire regime.

(Reprinted: Miller, C., and Urban, D.L. 1999. *Ecosystems* 2:76-87.

Climate change may affect forest fires either directly through the risk associated to weather conditions and/or through the impacts of climate change on vegetation. The paleo record and historical data show that changes in wildfire frequency are closely linked to changes in climate (Swetnam, 1993). Several studies tracking trends over the past century have found that fire frequency (Brown and Swetnam, 1994) and area burned correlated with temperature. Temperature and precipitation influences how a wildland fire burns on a time scale of hours to day by influencing the moisture content of the live and the dead vegetation (i.e., fuel) and the amount of heat transfer required for combustion of those fuels. On a time scale of weeks to months, climate continues to influence drought and the duration of the fire season. A short fire season provides fewer opportunities for fires to occur than a does a long fire season, thereby influencing the fire frequency of site. On longer time scales of years to decades, climate can influence fire regimes by governing plant distributions, growth rates, and the type and amount of fuel that result.

PROBLEM STATEMENT

One of the consequences of climate change will be an increase in the wildfire risk potential and this increase will be related to changes in precipitation and temperatures. Fires are strongly influenced by moisture content of the fuel. In forests most of the fuel consists of deal material, so once this material becomes dry the risk of fires increases. In addition to an increase in the number of days when forest fuel is dry enough to ignite; drought can also increase the amount of fuel that is available to burn. Therefore fire activity for an entire fire season is primed to increase with severe drought conditions. In the remainder of this thesis, how the forests are drying as a result of drought and increasing temperatures and how the fire risk is likely to change over the 21st century will be studied through the climatic indicator, Keetch and Byram's Drought Index (KBDI).

OBJECTIVES AND HYPOTHESES

The objectives that this research will address are:

O1: Investigate how high (A1fi) and low (B1) Carbon dioxide emission scenarios affect temperature and precipitation in Sequoia National Park for the 21st century?

H1a: Temperature will increase under both emission scenarios

- increases will be greater under higher emission scenario

H1b: Precipitation will decrease under both emission scenarios

- decreases will be greater under higher emission scenario

O2: Model how these climate changes will affect droughts in Sequoia National Park

H2: Droughts will increase under both emission scenarios

- increases will be greater under higher emission scenario

O3: Estimate the wildfire risk potential for Sequoia National Park under each emission scenario

H3: Wildfire risk potential will increase

- increases will be greater under higher emission scenario

DROUGHT INDEX AS A MEASURE OF FOREST FIRE HAZARD

A drought may be defined as an interval of time, generally of the order of months or years in duration, during which the actual moisture supply at a given place rather consistently falls short of the climatically expected or climatically appropriate moisture supply. To forest management personnel concerned with wildland fire, drought may mean a situation in which fuels are drier and fires are more intense than normally expected. Under drought conditions, more fuel is available resulting in the burning of ground fuels, whereas under normal conditions, only the surface fuels would burn [Ground fuels include the duff and litter on the soil surface and generally do not contribute to wildfire spread or intensity. Surface fuels include all dead and down woody materials, grasses, other herbaceous plant materials, and short shrubs, which are often the most hazardous fuels in many forests]. This is particularly likely in forests where vegetative species composition, density, and structure have been influenced by decades of fire suppression. The result is more intense fires and increased difficulty with suppression efforts. The amount of fuel that is available for combustion in a given fire (available fuel) is determined largely by the amount of water in the fuel (fuel moisture). Fuel moisture affects all aspects of fire behavior and fire effects: spread rate, intensity, smoke production, fuel consumption, and plant mortality.

Several indexes are available to track drought, including Palmer's drought index (1965) and crop moisture index (1968). The Energy Release Component (ERC) and the moisture content of large woody (1000-h) fuels from the U.S NFDRS and the Drought

Code and Duff Moisture Code from the Canadian FWI System are also used to indicate drought conditions. Keetch and Byram (1968) designed a drought index specifically for fire potential assessment. It is a number representing the net effect of evapotranspiration and precipitation in producing cumulative moisture deficiency in deep duff and upper soil layers. It is a continuous index, relating to the flammability of organic material on the ground. The index increases for each day without rain (the amount of increase depends on the daily high temperature) and decreases when it rains. The scale ranges from 0 (no moisture deficit) to 800. The range of the index is determined by assuming that there is 8 inches (20 cm) of moisture in a saturated soil that is readily available to the vegetation. For different soil types, the depth of soil required to hold 8 inches (20 cm) of moisture varies. A prolonged drought (high KBDI) influences fire intensity largely because more fuel is available for combustion (i.e. fuels have a lower moisture content). High values of the KBDI are an indication that conditions are favorable for the occurrence and spread of wildfires, but drought is not by itself a prerequisite for wildfires. Other weather factors, such as topography, wind, temperature, relative humidity and atmospheric stability, play a major role in determining the actual fire danger. The index's relationship to fire is that as the index value increases, the vegetation is subjected to greater stress because of moisture deficiency. At higher values, living vegetation dies and becomes fuel, and the duff/litter layer becomes more susceptible to fire.

Keetch-Byram Drought Index (KBDI)

The KBDI, specifically developed to equate the effects of drought with potential fire activities, is the most widely used system by fire managers in the southeastern United States. The index relates current and recent weather conditions to potential or expected fire behavior. The index value ranges from 0 to 800. This number is related to moisture deficit; a value of 0 defines a point of no moisture deficiency and 800 define the maximum drought possible for a particular location. The index indicates deficit inches of water in the soil. A KBDI reading of 300 means there is a deficit of 3.0 inches (8 cm) of ground water available to the vegetation. Prolonged droughts (high KBDI) influence fire intensity since more fuel is available for quick combustion (i.e. fuels have a lower moisture content). In addition, dry organic material in the soil can lead to increased difficulty in fire suppression. The purpose of the drought index is to provide fire control managers with a continuous scale of reference for estimating deep-drying conditions in areas where such information may be useful in planning fire control operations.

The effect of drought on forest fire behavior varies with fuel types and topographic conditions. Southern pine fuel will react differently to drought than mountainous hardwood fuels and consequently fire behavior will differ. The following co-relation of KBDI numbers with the fire behavior was primarily designed for the Southern Coastal Plains and Piedmont regions (the plateau between the coastal plain and the Appalachian Mountains: parts of Virginia and North and South Carolina and Georgia and Alabama) but can be considered applicable in many areas of the country. This index was added to the 1988 National Fire Danger Rating System (NFDRS) specifically designed for use in forest management in the eastern and western United States (Melton, 1989). However, an initial KBDI value must be defined to begin the calculations. This is particularly troublesome for stations at which observations are not taken all year long. Keetch and Byram caution that it is essential to begin the drought calculations for a particular location from a time at which the upper soil layers are completely saturated with water. This condition is assumed to be met right after snowmelt for areas receiving heavy snowfall, or right after substantial rains.

Co-Relation of KBDI Values with Potential Fire Behavior

The KBDI value correlates with potential fire behavior as follows (Melton, 1989)

0 - 200 Soil and fuel moisture are high and do not contribute significantly to fire intensity. Most fuels will not readily ignite or burn. Nearly all soil organic matter, duff, and litter are left intact. Even if these layers are not fully saturated with water, they will resist ignition. Some fuel types like grasses burn actively. With sufficient sunlight and wind, cured grasses and some light surface fuels will burn in spots and patches.

200 - 400 Fires burn more readily. Heavier fuels will still not readily ignite and burn. Lower litter and duff layers are drying and beginning to contribute to fire intensity. The increase in fuel consumption and intensity can result in heavier fuel classes becoming involved in the burn. Soil exposure is minimal. Patched of unburned vegetation are still common, but these conditions tend to allow for more smoldering and creeping fires that may eventually consume more surface fuels.

400 - 600 Very intense fires can be generated with burns ignited in this range of conditions. Under these levels, most of the duff and associated organic layers will be sufficiently dry to ignite and contribute to the fire intensity and will burn actively. The intensity can be expected to increase at an almost exponential rate from the lower to he upper ends of this range. These 400-600 levels indicate the increase in fuel availability for consumption and consequently increase the fire's intensity.

600 - 800 The 600-800 range of the KBDI represents the most severe drought conditions identified within the index and results from an extended period of little or no precipitation and high day time temperatures. The index is associated with severe drought, increased wildfire occurrence, intense and deep burning fires. Live fuels burn actively. Fires will burn thorough the night and heavier fuels will actively burn and contribute to fire intensity. Once ignited, the large fuel classes with burn intensely. These fires are very difficult to control and contain.

Keetch-Byram Drought Index and Vegetation Cover

The physical theory for the KBDI is based on the following assumptions:

- the rate of moisture loss in an area depends on the vegetation cover in that area
- the vegetation cover in turn (and therefore its transpiration capacity) depends on the mean annual rainfall.
- the rate of moisture loss is thus a function of the mean annual rainfall. Therefore, the rate of moisture loss decreases with decreasing vegetation cover, hence, with decreasing mean annual rainfall.

Table 1 emphasizes the importance of the relationship between vegetation cover, mean annual rainfall, and KBDI.

Table 1: Consecutive drying days needed to reach KBDI of 500 (Keetch and Byram, 1968).

Area	Mean Annual Rainfall (inches)	Consecutive number of drying days needed to reach KBDI of 500
A	10-19	157
B	20-29	109
C	30-39	78
D	40-59	52
E	60 or more	36

Consider the two extremes in the above table. If area A and E both started with KBDI=0 on May 31, then the area E with heavy rainfall would reach KBDI=500 in 36 consecutive days, and area A with light rainfall would reach the same stage in 157 consecutive days. This implies that area A would have less vegetation cover (hence less available fuel for fire) due to lower mean annual rainfall and will require more drying days to reach a KBDI value of 500.

Keetch-Byram Drought Index Calculations

To begin the calculations, an initial KBDI value must be defined. This can be done by finding a day at the location of interest when the index is likely to have a value at or near zero. This means that an observer starting a drought index record cannot automatically begin at zero. The zero point may have occurred weeks or months before, or even during the previous year. It is necessary to go back in time until a day is reached on which it is reasonably certain that the upper soil layers were saturated, then bring the record forward day by day to the starting date. In areas of heavy snowfall, it is normally safe to assume saturation just after the snow melts in the spring. When starting a record in snow-free areas, it is necessary to go back to a period of abundant rainfall, such as 6 or 8 inches in a period of a week. The index must be very low, if not actually zero, at the end of the rainy period (Keetch and Byram, 1968).

The input parameters for KBDI are daily rainfall (inches), daily maximum temperature (degrees Fahrenheit), and the mean annual rainfall (inches). The daily precipitation decreases the KBDI, and the daily maximum temperature increases the KBDI. The KBDI uses the maximum temperature as a proxy for evaporation. The temperature factor has no effect unless the day's maximum temperature is above 50^0F (10^0C). The second step involves subtracting a factor of the daily precipitation from the previous day's KBDI. The daily precipitation, measured in inches, is multiplied by a 100. If less than 0.2 inches of rain fell during the previous day, the model subtracts 0.2 from the current day's precipitation. The daily precipitation is set to zero if it is less than 0.2 inches. If the KBDI is below zero (after subtraction), the index is set to zero (Keetch and Byram 1988). The third step involves increasing the drought index by a drought factor. The drought factor dQ increases with higher daily temperatures and is calculated using the equation below

$$dQ = [800-Q]\,[0.968\exp(0.0486T) - 8.30]\, dt * 0.001 / [1+ 10.88\exp(-0.0441R)] \quad \text{eq (1)}$$

where, T is the daily maximum temperature,

R is the mean annual rainfall,

Q is the current KBDI, and

dt is a time increment set equal to one day.

AN OVERVIEW OF FIRE AND DROUGHT IN THE SIERRA NEVADA

The reduction in area burned in the 20^{th} century, combined with the effects of forest management practices, has lead to substantial increase in quantity and changes in arrangement of live and dead fuels (McKelvey, 1996). The impact of forest management in the form of fire suppression in the 20^{th} century has lead to the accumulation of dead fuels on the forest floor in excess of their pre-settlement levels. Also, logging on forest service and private lands, combined with no treatment of slash, increases the vulnerability of stands to damage from wildfires (Weatherspoon, 1996). Thus, compared to the pre-settlement conditions, trees in the current Sierra Nevada forests are generally younger, denser, smaller in diameter, and more homogenously distributed. There is increased fuel available for combustion on many sites and these conditions create forests that are more likely to support large, severe fires.

The overall fire pattern in Figure 4 suggests that weather may have an influence on acreage burned. In the 1920s, 1930s, the late 1950s and the 1980s—all periods that we would associate with drought—there were increases in fire acreage (McKelvey and Busse, 1996).

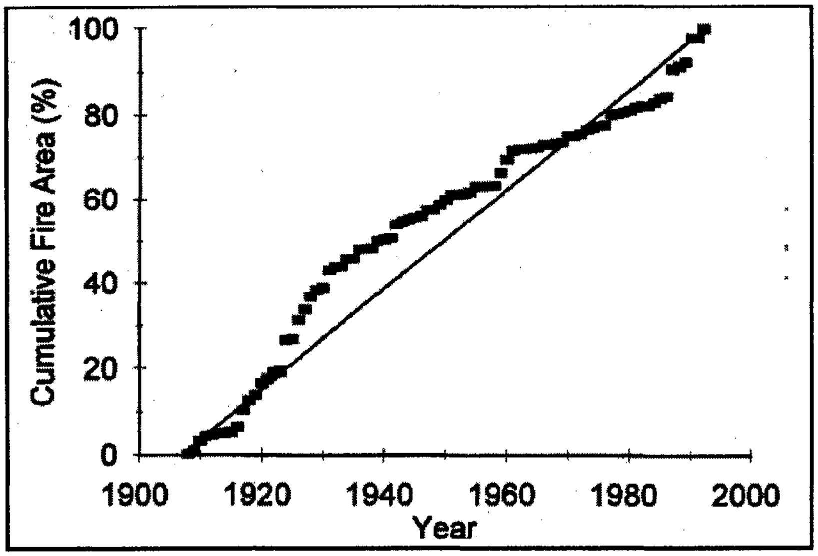

Figure 4: 20th century fire pattern on forest service lands

Cumulative fire area burned between 1908 and 1992. The line represents the rate of increase, assuming a constant area burned per year.

(Reprinted from: McKelvey, K.S., and Busse, K.K. 1996).

McKelvey and Busse (1996) built a simple drought index of cumulative temperature minus cumulative precipitation to study the relationship between temperature, precipitation, drought (KBDI) and wildfires. The results showed that all of extreme fire years in the Sierra Nevada occurred during years that were hot and dry (Figure 5) (see also Swetnam and Baisan, 2003). Nineteen eighty seven was an extreme fire year for the Sierra Nevada having more drought days at all elevations. The fall fire season of 1987 had Keetch-Byram Drought Index (KBDI) level readings in excess of 700 through November falling into the 600 level in December.

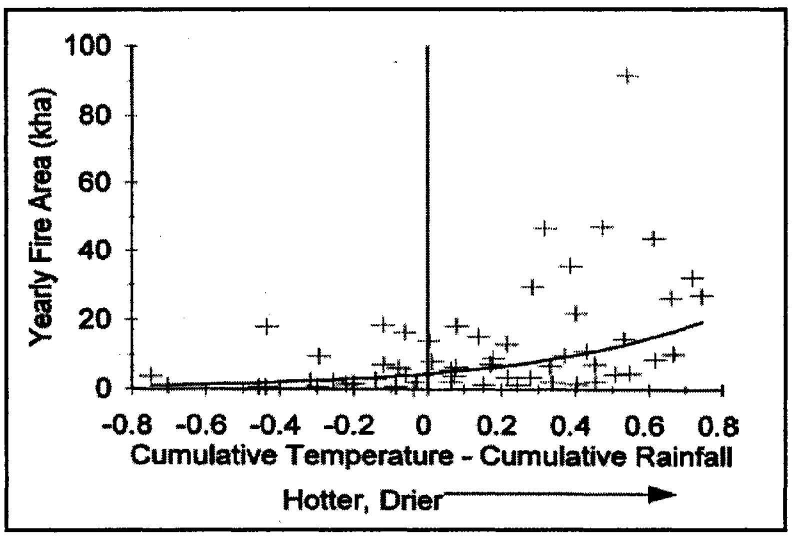

Figure 5: Average number of drought days (KBDI) per season for 132 stations in and around Sierra Nevada for the period 1979-89

(Reprinted from: McKelvey, K.S., and Busse, K.K. 1996).

METHODS

Study Site

The study site is 2135 m elevation in the Sequoia National Park (118^{0}45′ W, 36^{0}35′ N) in the southern Sierra Nevada, east of Fresno, California. The park was the second national park to be formed in the USA, in 1890 and spans 404,051 acres (1,635 km^2). The park is adjacent to Kings Canyon National Park; the two are administered by the National Park Service as one unit, called Sequoia and Kings Canyon National Parks. The park spans a broad range in elevation: the Ash Mountain entrance is at 1700 ft (518 m) elevation, while approximately 35 miles (56 km) east, Mount Whitney attains 14,491 ft (4,417 m), the highest point in the continental USA

Sierra Nevada as Study Site

California is a useful case study for climate change impacts because wildfire is of critical economic and ecological importance in the state. More than half of the most economically damaging fires in the US over the past 170 years occurred in California (Fried et al, 2004). Fire is among the most important forces shaping the California's forest and rangeland ecosystems. Fire was historically a principal mechanism by which the nutrients contained in wood fuels were recycled. Due to the extensive and successful application of fire suppression during the last century, rates of biomass recycling have declined and fuels have accumulated throughout most wildland, thus increasing fuel loads and potential fire severity and rate of spread (Weatherspoon, 1996). Fuel conditions in much of the Sierra Nevada support the potential for large, severe fires (Sapsis et al. 1996). Climate and fire histories reconstructed from tree ring chronologies have established that fire regimes are directly related to climatic factors in Sierra Nevada (Swetnam, 1993).

Climate Model Projections for the Study Site

This study is based on climate projections resulting from the SRES (Special Report on Emission Scenarios) for the lowest (B1≈ 550 ppm CO_2 in 2100) and highest (A1fi ≈ 970 ppm CO_2 in 2100) Intergovernmental Panel on Climate Change (IPCC) emission pathways (Nakicenovic et al. 2000). Two Global Climate models, the low-sensitivity National Center for Atmospheric Research/Department of Energy Parallel Climate Model (PCM) (Washington et al. 2000) and the medium-sensitivity U.K. Met Office Hadley Center Climate Model, Version 3 (HadCM3) (Gordon et al. 2000; Pope et al. 2000) were used to project monthly temperature and precipitation data for these emission scenarios, after bias correction and statistical downscaling to a 1/8 degree grid (Hayhoe et al. 2004). The bias corrected and downscaled monthly data has been further downscaled to daily data for Sequoia National Park by randomly re-sampling from the historical record using the gridded observed daily meteorological data from 1915-2003 (Hamlet and Lettenmaier, 2004). The observed data were aggregated to monthly and averaged over a domain including all of the met station locations included in the analysis. For each month, threshold values were determined to divide the record into dry-cool, dry-warm, wet-cool, and wet-warm. The projected monthly values (1960-2099) were then placed into the appropriate category and a historic year in the same category was randomly selected and rescaled so the monthly precipitation and temperature (average) matched the projected value.

The HadCM3 and PCM projections for this location are made at an elevation of 2135 m for a period of 1970-2099. Using these daily temperature and precipitation projections, the Keetch/Bryam Drought Index (KBDI) will be calculated for the Park for the 21st century. The results will be summarized in the form of histograms, with number of days greater than a threshold KBDI (300, 350, 400, 500, and 600).

The histograms will be plotted for the periods 1970-1999, 2020-2049, and 2070-2099 for the months of July, August, and September. Consistently high daily temperature, averaging more than 21^{0}C, is needed for the development of an appreciable drought (Keetch and Byram, 1968). The development of severe or appreciable drought at these temperatures is mainly limited to the period June-September in western United States. Therefore, this study computed the KBDI for the months June-September during the 21st century to study the wildfire risk.

Input Parameters for KBDI Calculations

- As mentioned in the physical theory of KBDI calculations, "current day's" KBDI is computed by the addition of yesterday's drought index and a drought factor. This cumulative feature means that computation of KBDI for the 21st century cannot automatically begin, and that it needs a starting KBDI value recorded in the past for the location of interest. This starting KBDI value was acquired for

January 1, 1960 from NOAA (National Oceanic and Atmospheric Administration) for a location called "Grant Grove" (36°44'N, 18°58'W) within the park. This location is at an elevation of 2011.4 m (Source: Pasha Groisman, NOAA).

- Also as mentioned in the theory of KBDI, the KBDI value of a particular location depends on the vegetation cover of that area, which in turn is a function of the mean annual rainfall for that place. This study assumes that the vegetation cover does not change during the study period, which is during the 21st century. Hence to be consistent with the assumptions and concept of KBDI calculations, the mean annual precipitation of 1970-1999 has been used for calculating KBDI. Incorporating different mean annual precipitation for different periods would mean that the vegetation cover and characteristic will change over that period and will introduce a bias in the results. The model (HadCM3 and PCM) projections were used for the daily temperature and precipitation data.

CLIMATE MODELS AND EMISSION SCENARIOS

Using Emission Scenarios to Develop a Plausible Range of Outcomes

To forest management personnel concerned with wildland fire, it is essential to have knowledge of the full range of potential changes in wildfire, for planning in the future. To this end, the intention of this analysis is to provide the scientific and management community with model projections for wildfire risk in the 21st century based on the SRES emission scenarios (Nakic´enovic´ et al, 2000). The IPCC commissioned the Special Report on Emission Scenarios (SRES) to broaden assessments to include a range of outcomes and to focus analysis on a coherent set of scenarios to facilitate comparison. The scenarios produced by the SRES team rest on assumptions regarding economic growth, technological developments, and population growth, which are arguably the three most critical variables affecting the uncertainty over future climate change and policy options. The scenarios assist in climate change analysis, including climate modeling and the assessment of impacts, adaptation, and mitigation. The six scenario groups – the three scenario families A2, B1, and B2, plus three groups within the A1 scenario family, A1B, A1FI, and A1T – and four cumulative emissions categories were developed as the smallest subsets of SRES scenarios that capture the range of uncertainties associated with driving forces and emissions. This study considers the A1fi and B1 emission scenarios.

- The A1fi scenario is a fossil-fuel intensive scenario lying at the high end of the range of SRES GHG emissions pathways throughout the 21st century. In this scenario, a rapid rate of temperature change in driven by a continued dependence on fossil fuels for economic development.

- The B1 scenario, which has the lowest emissions during the 21st century, focuses on global solutions to economic, social, and environmental sustainability. Clean and efficient technology like renewable sources of energy is introduced. However, no specific climate initiatives are taken

Climate Modeling

Modeling provides a tool to understand how forests respond to climate change across large spatial and temporal domains. A climate model is a set of mathematical statements describing physical, biological, and chemical processes that determine climate. The simplest models involve just a few fundamental equations and a host of simplifying assumptions. Most sophisticated are the large-scale computer models known as General Circulation Models (GCMs). GCMs are often used to project the spatial distribution of change in climatic conditions. Despite their coarse spatial and temporal resolution, GCMs provide the best means currently available to project future climate and forest fire danger on a broad scale.

Output from the Parallel Climate Model (PCM) and Hadley Centre Climate Model, version 3 (HadCM3) will be used in this study. These are three-dimensional climate models, with a resolution of 2.5° latitude by 2.5° longitude for PCM and 2.5° latitude by 3.75° longitude for HadCM3. HadCM3 is a coupled atmosphere-ocean general circulation model (AOGCM) developed at the Hadley Centre and described by Gordon et al (2000) and Pope et al (2000). Unlike earlier AOGCM's at the Hadley Centre and elsewhere (including HadCM2), HadCM3 does not need flux adjustment (additional "artificial" heat and freshwater fluxes at the ocean surface) to produce a good simulation.

Global temperatures are projected to increase by 1.4^0C to 5.8^0C by 2100 (IPCC, 2001). It is certain that precipitation will change, with some regions becoming drier and others wetter. Projected intensification of the hydrological cycle increases the threat of more floods, although how this intensification will affect different regions is likely to vary considerably. Likewise, changes in precipitation patterns bring the threat of more extreme droughts to some regions while others may experience fewer droughts or even floods. Regional changes in climate are more difficult to predict than global, because the extrapolation from global to local scales is not precise. In particular, these models lack sufficient spatial resolution to capture the drivers of local climate variations such as mountain ranges or lakes. However, these results still allow for determination of general trends across the region of interest.

RESULTS AND DISCUSSIONS

Table 2 shows the 5-year running mean temperature simulations and projections for the four models for August and September. The results show higher mean temperatures (in deg C) during 2070-99 as compared to 2020-2049 and 1970-99. See Figures 6-13. The highest temperature increase is for HadCM3-A1fi and lowest for PCM-B1. [Note: The 5-year running mean of data is implemented to smooth out possible variations]

Table 2: 5-year running mean (RM) temperature (deg C) for the four models for the 21st century for Sequoia National Park ($118^0 45'$ W, $36^0 35'$ N and elevation 2,135 m).

MODELS		1970-1999 Simulations	2020-2049 Projections	2070-2099 Projections
	Months	**5-yr RM Mean Tmax**		
HadCM3-A1fi	August	19	25	30
	September	16	21	26
HadCM3-B1	August	19	24	27
	September	16	20	22
PCM-A1fi	August	19	22	25
	September	16	20	23
PCM-B1	August	19	23	23
	September	16	19	21

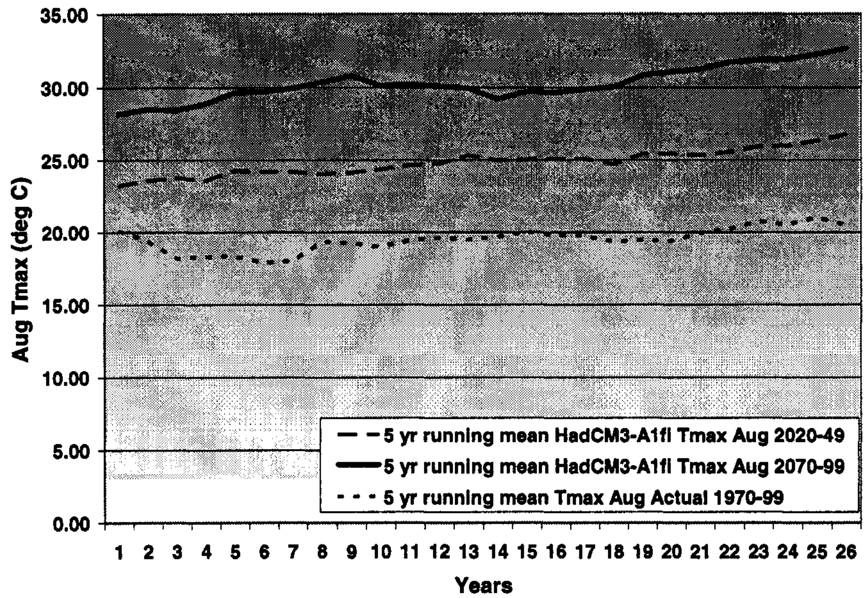

Figure 6: August Tmax (deg C) for HadCM3-A1fi for 2020-49 and 2070-99 for Sequoia National Park (118^{0}45′ W, 36^{0}35′ N and elevation 2,135 m).

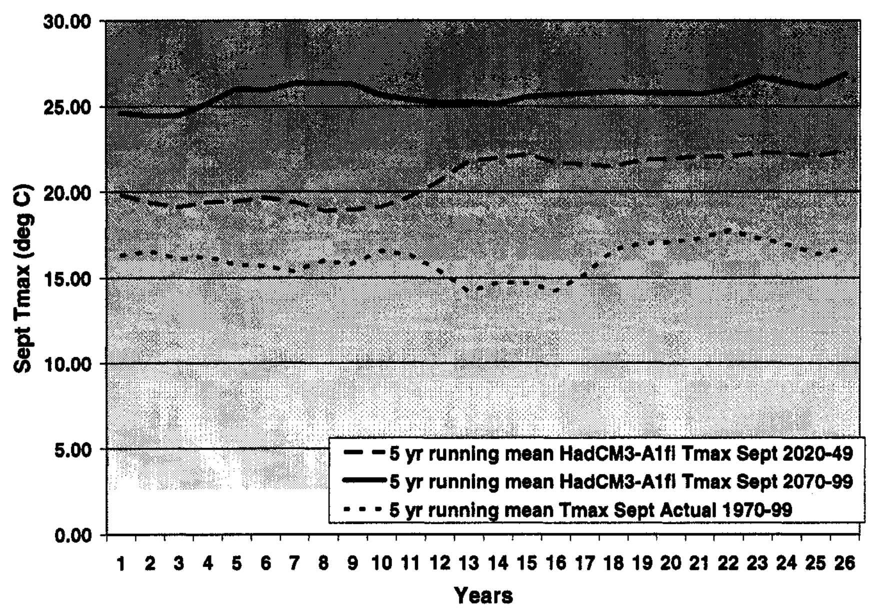

Figure 7: September Tmax (deg C) for HadCM3-A1fi for 2020-49 and 2070-99 for Sequoia National Park (118^{0}45′ W, 36^{0}35′ N and elevation 2,135 m).

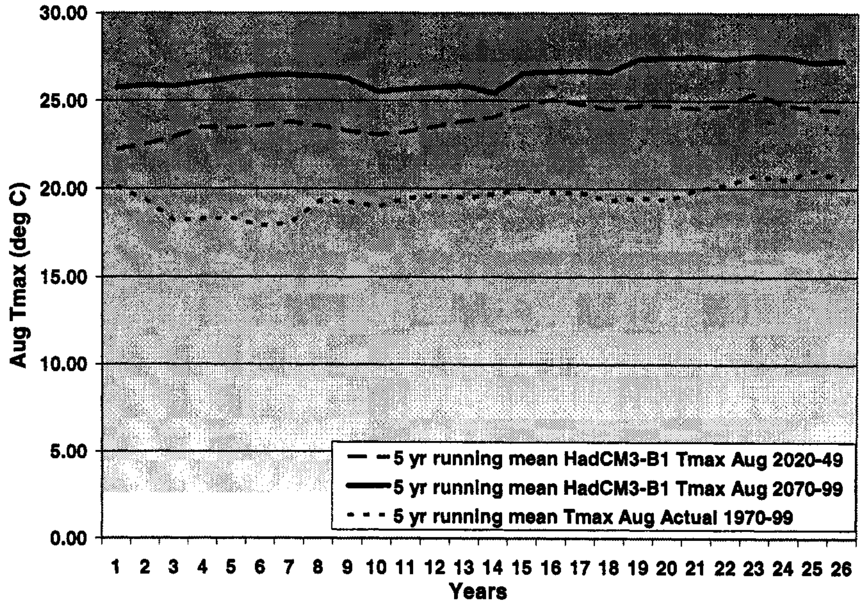

Figure 8: August Tmax (deg C) for HadCM3-B1 for 2020-49 and 2070-99 for Sequoia National Park ($118^0 45'$ W, $36^0 35'$ N and elevation 2,135 m).

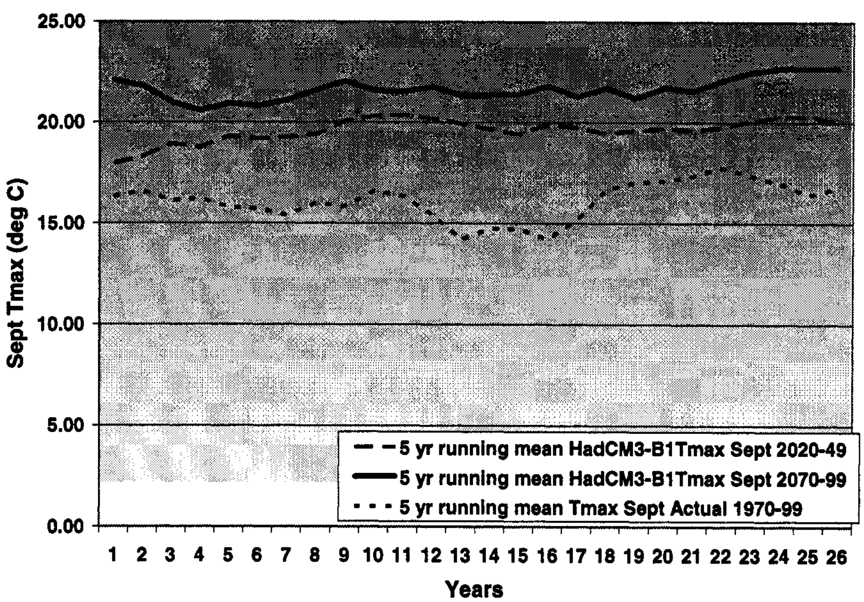

Figure 9: September Tmax (deg C) for HadCM3-B1 for 2020-49 and 2070-99 for Sequoia National Park ($118^0 45'$ W, $36^0 35'$ N and elevation 2,135 m).

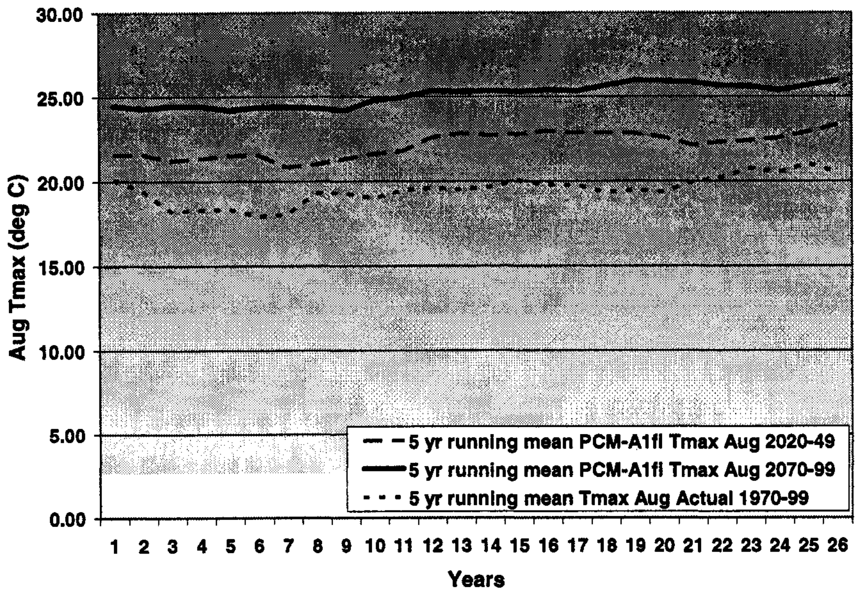

Figure 10: August Tmax (deg C) for PCM-A1fi for 2020-49 and 2070-99 for Sequoia National Park (118^{0}45′ W, 36^{0}35′ N and elevation 2,135 m).

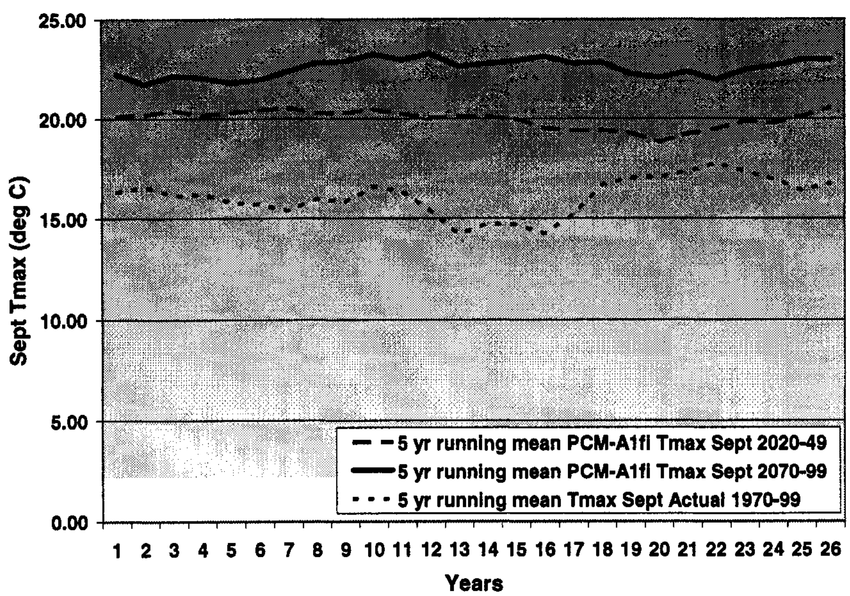

Figure 11: September Tmax (deg C) for PCM-A1fi for 2020-49 and 2070-99 for Sequoia National Park (118^{0}45′ W, 36^{0}35′ N and elevation 2,135 m).

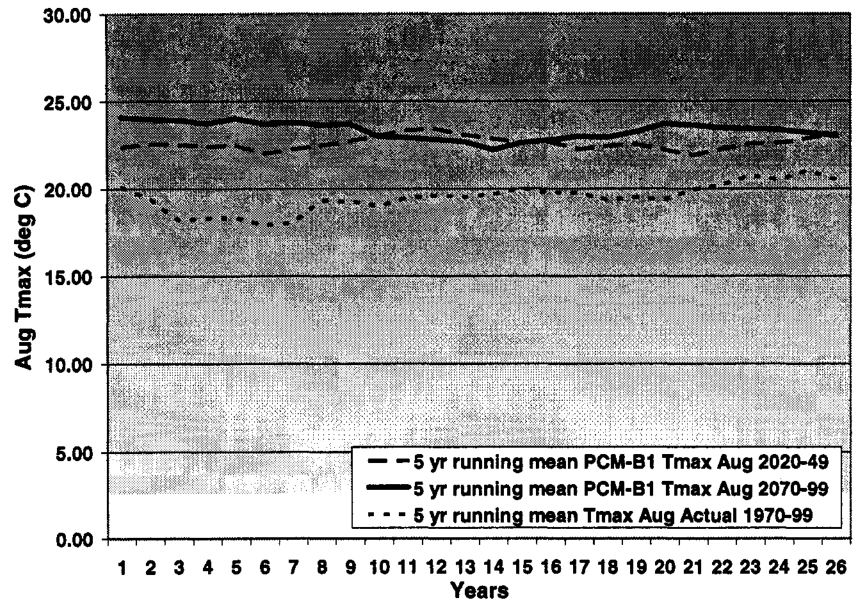

Figure 12: August Tmax (deg C) for PCM-B1 for 2020-49 and 2070-99 for Sequoia National Park ($118^0 45'$ W, $36^0 35'$ N and elevation 2,135 m).

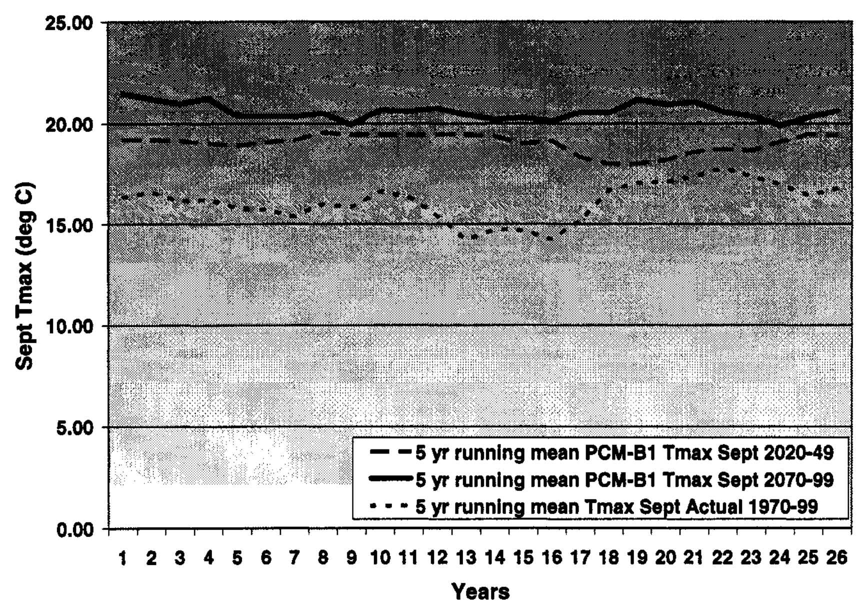

Figure 13: September Tmax (deg C) for PCM-B1 for 2020-49 and 2070-99 for Sequoia National Park ($118^0 45'$ W, $36^0 35'$ N and elevation 2,135 m).

Table 3 shows the 5-year mean precipitation (mm) simulations and projections data for 1970-99, 2020-49 and 2070-2099 for August and September. Figures 14-21 show that precipitation shows a tendency towards slight decreases in the second half of the century with no obvious inter-scenarios differences in magnitude or frequency (except in case of HadCM3-B1, where it increases in September from 1.2 mm to 1.6 mm). The precipitation increases during the mid-century (2020-49) for September for all models and emission scenarios, the highest being for HadCM3-A1fi. *[Note: Mean annual precipitation is used to calculate the Drought Factor. The KBDI is calculated using the drought factor, daily temperature and daily precipitation for a particular location and duration, e.g. Sequoia National Park for 2020-49 and 2070-99].*

Table 3: 5-year running mean (RM) precipitation (mm) for all four models for the 21st century for Sequoia National Park (118^{0}45′ W, 36^{0}35′ N and elevation 2,135 m).

MODELS		**1970-1999 Simulations**	**2020-2049 Projections**	**2070-2099 Projections**
	Months	**5-yr RM Mean PPT**		
HadCM3-A1fi	August	0.2	0.1	0.1
	September	1.1	1.5	1.4
HadCM3-B1	August	0.2	0.2	0.3
	September	1.1	1.2	1.6
PCM-A1fi	August	0.2	0.1	0
	September	0.7	0.9	0.7
PCM-B1	August	0.2	0.2	0.1
	September	1.1	1.2	1.3

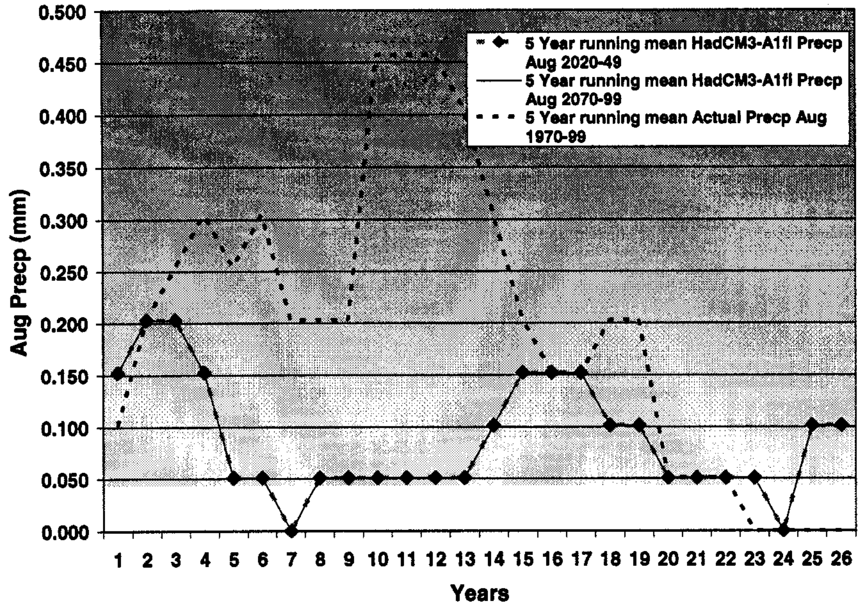

Figure 14: August precipitation (mm) for HadCM3-A1fi for 2020-49 and 2070-99 for Sequoia National Park (118^{0}45′ W, 36^{0}35′ N, elevation 2,135 m).

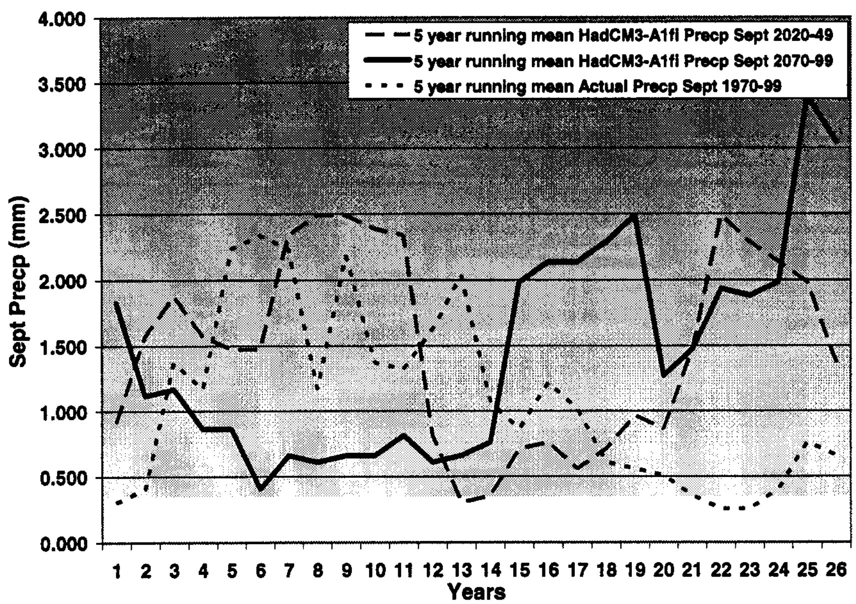

Figure 15: September precipitation (mm) for HadCM3-A1fi for 2020-49 and 2070-99 for Sequoia National Park (118^{0}45′ W, 36^{0}35′ N, elevation 2,135 m).

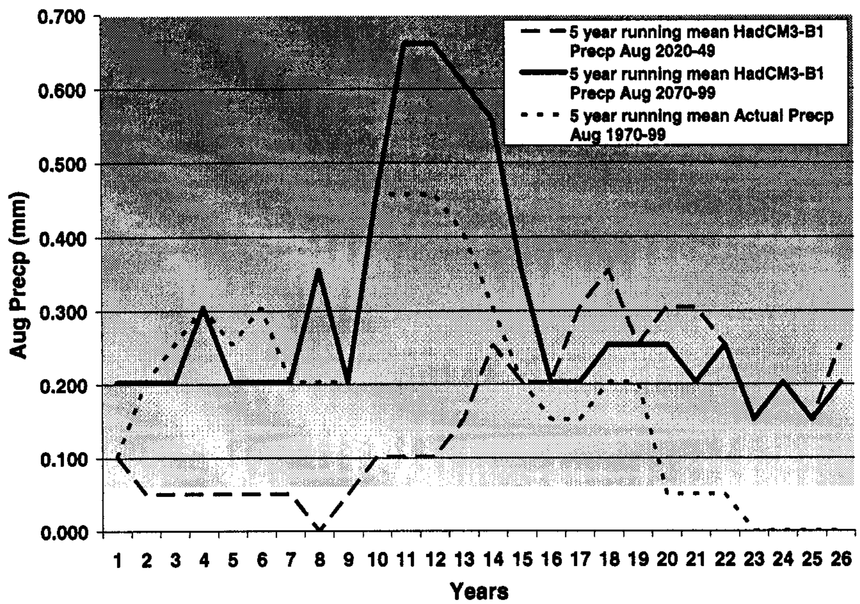

Figure 16: August precipitation (mm) for HadCM3-B1 for 2020-49 and 2070-99 for Sequoia National Park (118^{0}45′ W, 36^{0}35′ N, elevation 2,135 m).

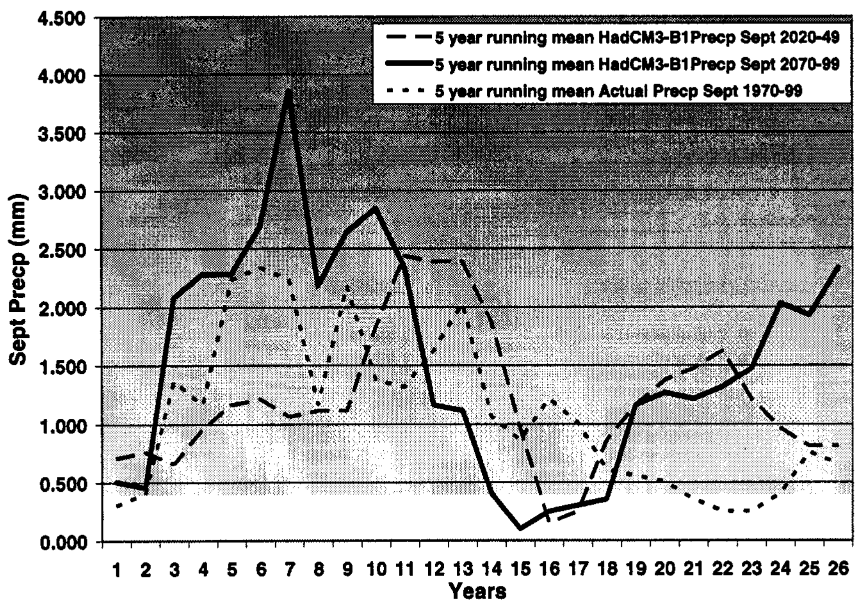

Figure 17: September precipitation (mm) for HadCM3-B1 for 2020-49 and 2070-99 for Sequoia National Park (118^{0}45′ W, 36^{0}35′ N, elevation 2,135 m).

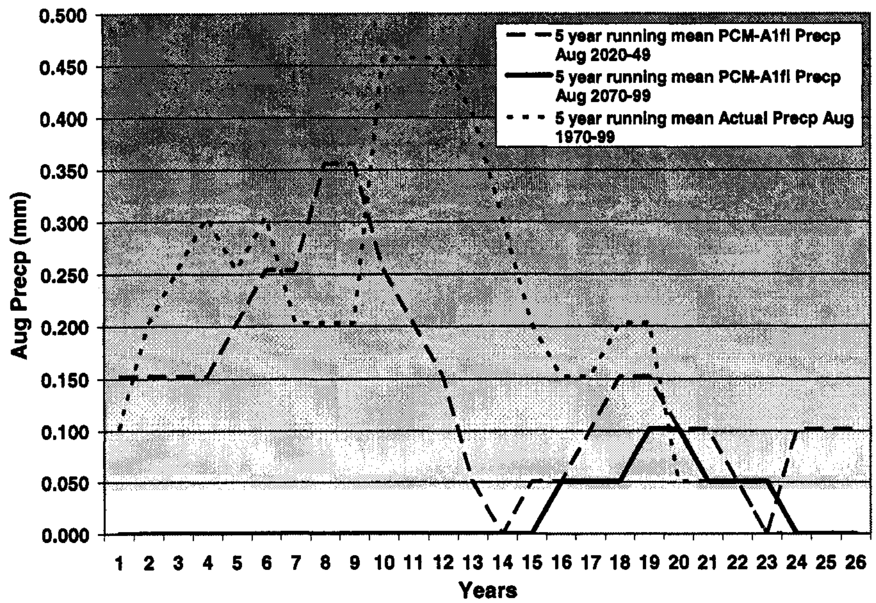

Figure 18: August precipitation (mm) for PCM-A1fi for 2020-49 and 2070-99 for Sequoia National Park (118^{0}45′ W, 36^{0}35′ N, elevation 2,135 m).

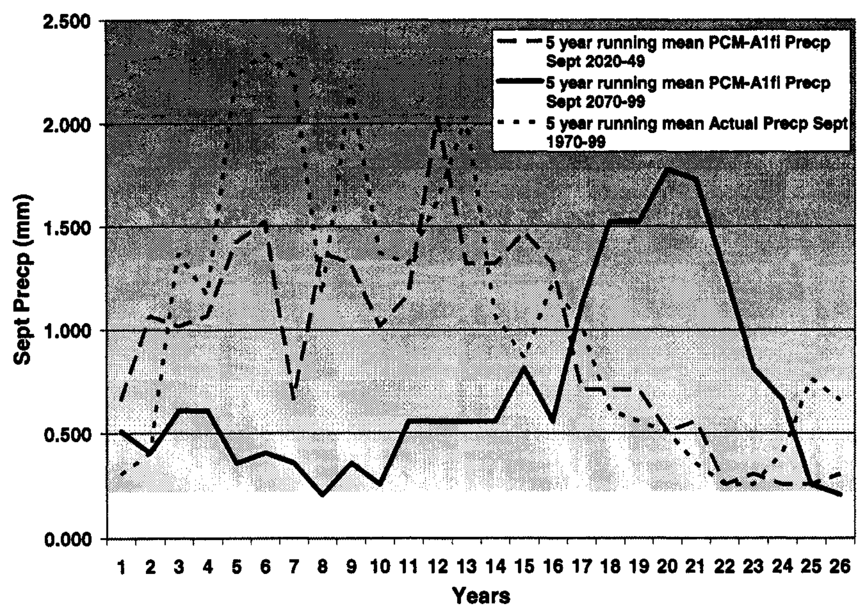

Figure 19: September precipitation (mm) for PCM-A1fi for 2020-49 and 2070-99 for Sequoia National Park (118^{0}45′ W, 36^{0}35′ N, elevation 2,135 m).

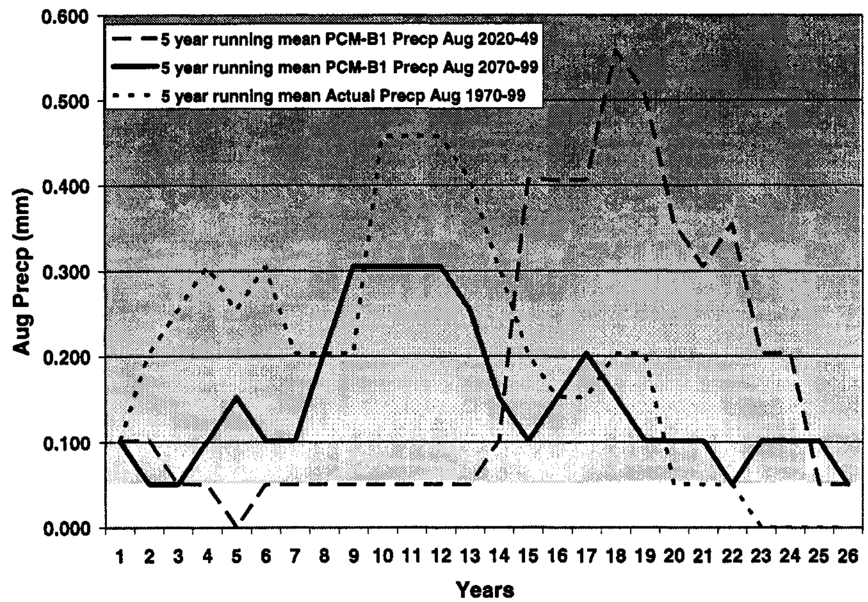

Figure 20: August precipitation (mm) for PCM-B1 for 2020-49 and 2070-99 for Sequoia National Park (118^{0}45′ W, 36^{0}35′ N, elevation 2,135 m).

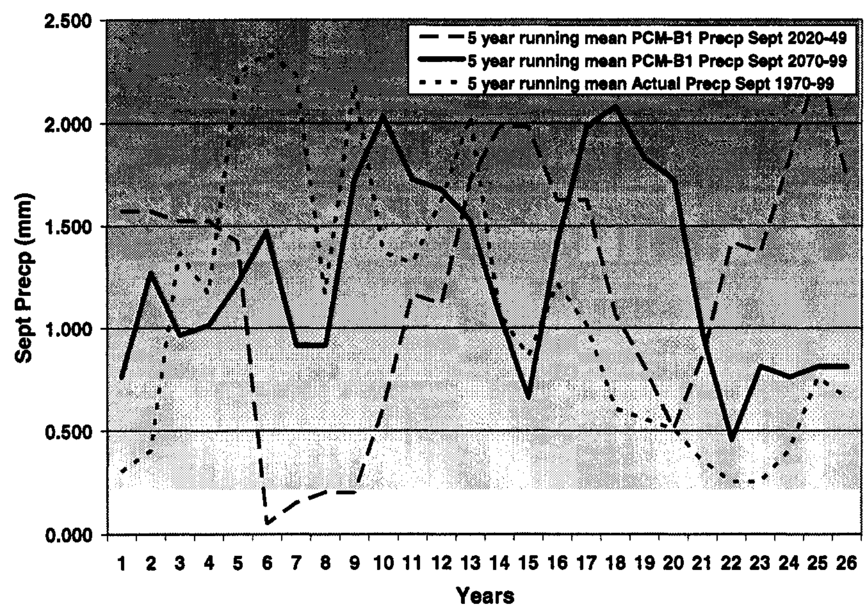

Figure 21: September precipitation (mm) for PCM-B1 for 2020-49 and 2070-99 for Sequoia National Park (118^{0}45′ W, 36^{0}35′ N, elevation 2,135 m).

Figures 22-25 show the 5-year running mean (RM) of KBDI data for all the four models from 2000-2099 for July, August, and September. The figures show that HadCM3-A1fi has higher mean values of KBDI and PCM-B1, the lowest. The KBDI value increases from July-September and is higher for 2070-99 as compared to 2020-49 (Table 4).

Table 4: 5-year running mean KBDI values for four models for July –September 2020-49 and 2070-99 for Sequoia National Park (118°45′ W, 36°35′ N and elevation 2,135 m).

MODELS 2020-2049	**Jul 5-yr RM KBDI**	**Aug 5-yr RM KBDI**	**Sept 5-yr RM KBDI**
HadCM3-A1fi	262.12	402.94	444.41
HadCM3-B1	241.93	738.63	426.56
PCM-A1fi	214.35	334.82	385.38
PCM-B1	217.51	347.93	395.15
MODELS 2070-2099	**Jul 5-yr RM KBDI**	**Aug 5-yr RM KBDI**	**Sept 5-yr RM KBDI**
HadCM3-A1fi	411.60	548.13	575.27
HadCM3-B1	329.03	473.61	507.13
PCM-A1fi	293.78	436.86	501.99
PCM-B1	231.55	361.00	407.48

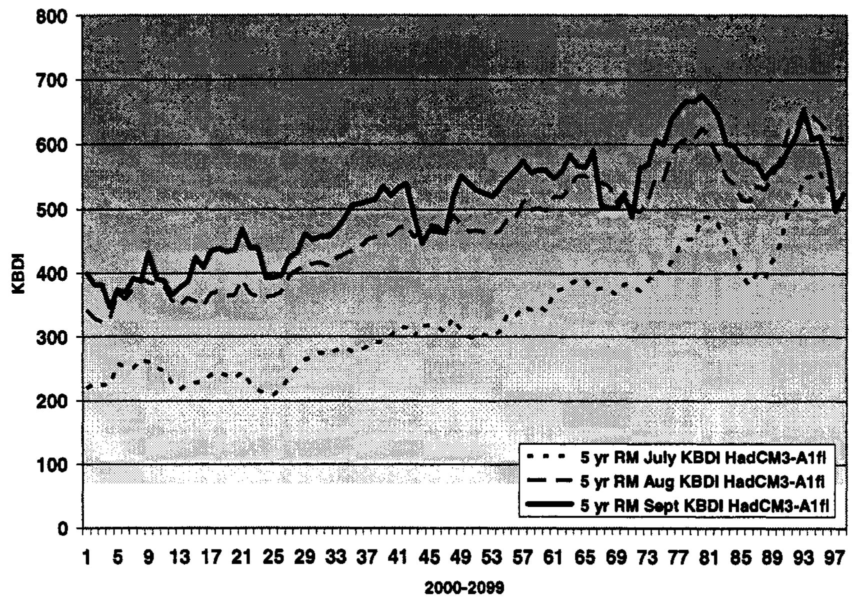

Figure 22: KBDI data for Sequoia National Park (118°45′ W, 36°35′ N and elevation 2,135 m) for 2000-2099 (July-Sept) for HadCM3-A1fi.

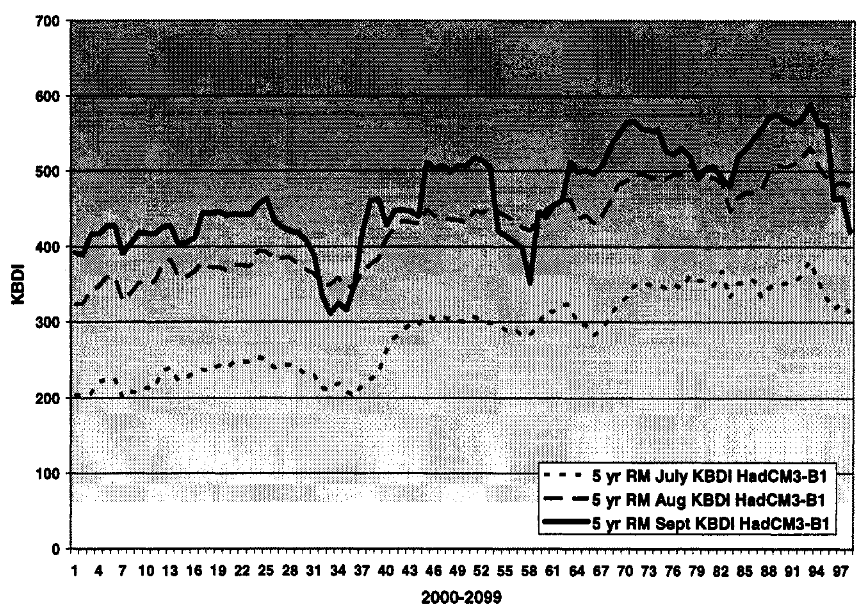

Figure 23: KBDI data for Sequoia National Park (118°45′ W, 36°35′ N and elevation 2,135 m) for 2000-2099 (July-Sept) for HadCM3-B1.

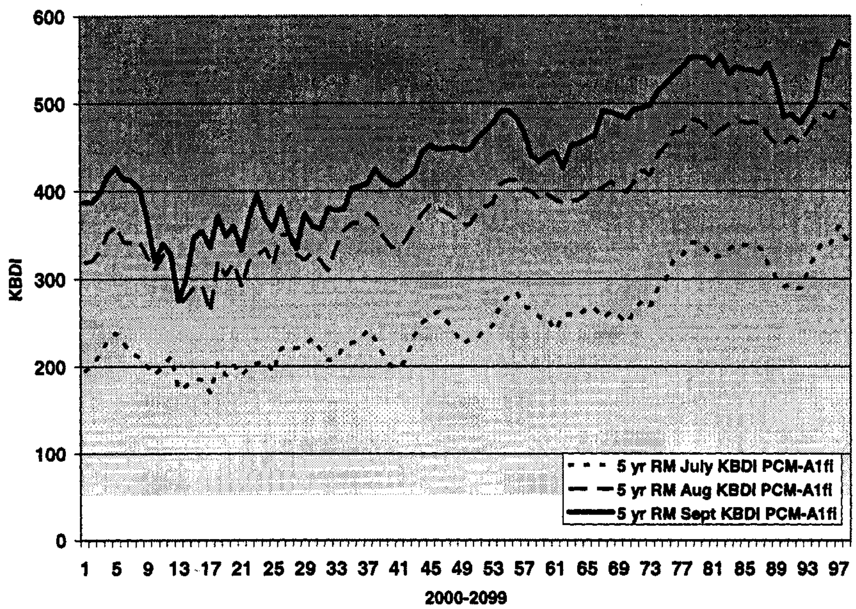

Figure 24: KBDI data for Sequoia National Park ($118^{0}45'$ W, $36^{0}35'$ N and elevation 2,135 m) for 2000-2099 (July-Sept) for PCM-A1fi.

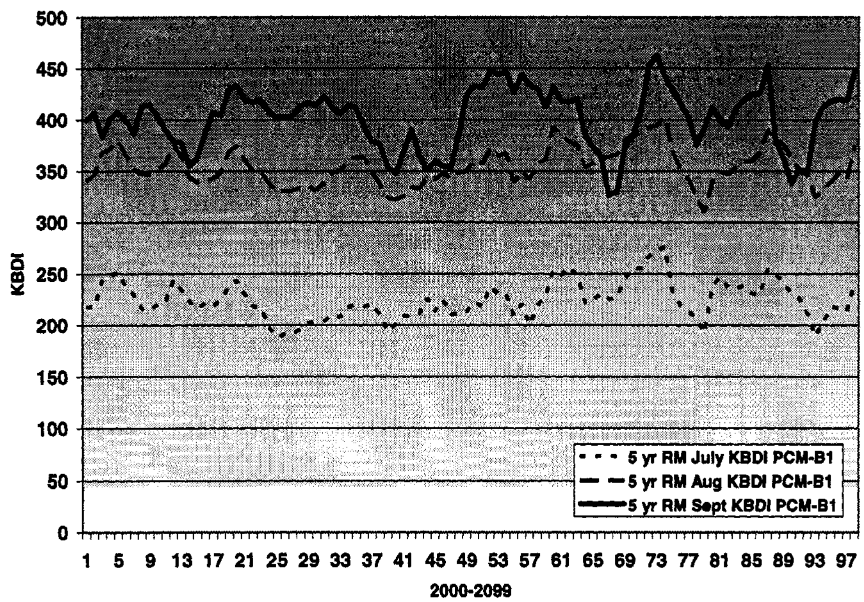

Figure 25: KBDI data for Sequoia National Park ($118^{0}45'$ W, $36^{0}35'$ N and elevation 2,135 m) for 2000-2099 (July-Sept) for PCM-B1.

Figures 26-28 show the 5-year running mean of KBDI values for all four models by month (for July, August, and September) for the period 2000-2099. The comparison for all three months shows that the value of KBDI increases from July to September. Also HadCM3-A1fi (high emission scenario, high sensitivity model) has the highest value of KBDI and PCM-B1 (lowest emission scenario, low sensitivity model) has the lowest value of KBDI.

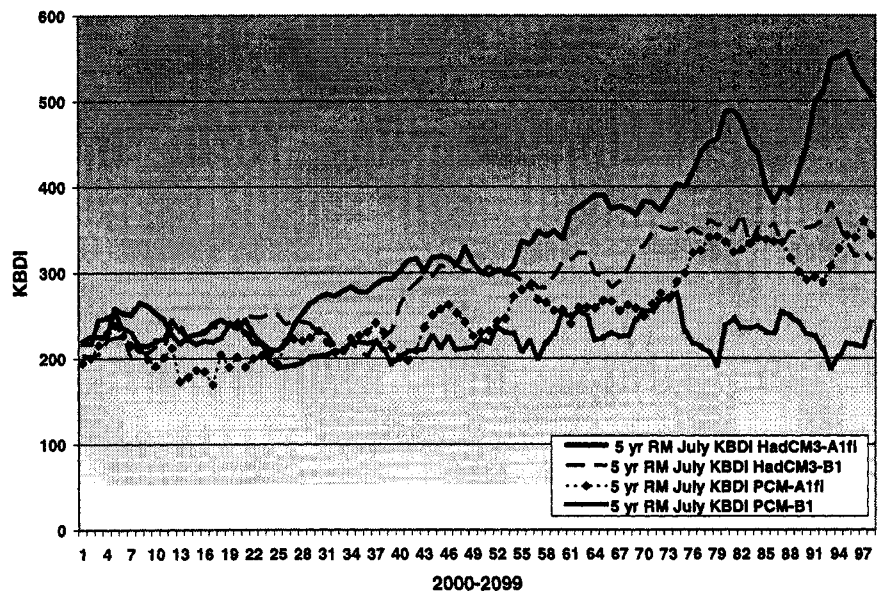

Figure 26: 5-year running mean of KBDI values for July, 2000-2099 for the four models for Sequoia National Park (118°45′ W, 36°35′ N, elevation 2,135 m).

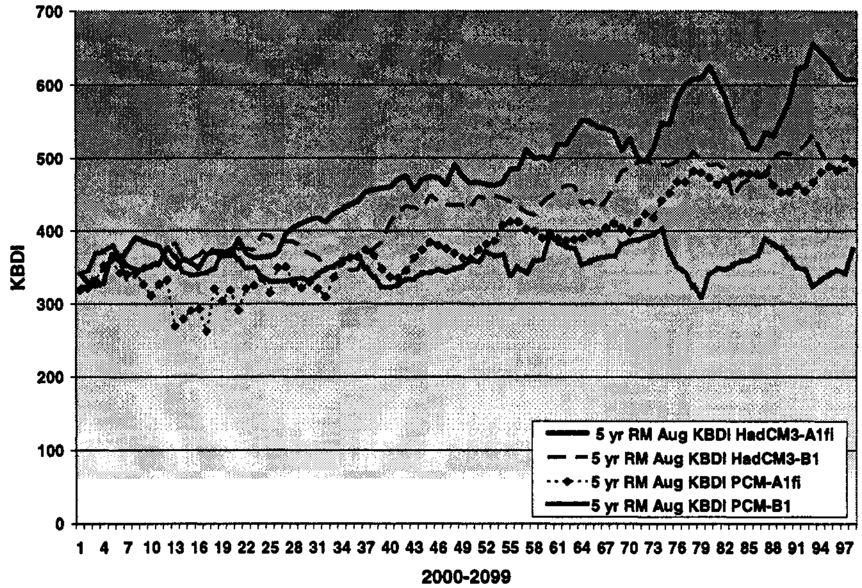

Figure 27: 5-year running mean of KBDI values for August, 2000-2099 for the four models for Sequoia National Park (118°45′ W, 36°35′ N, elevation 2,135 m).

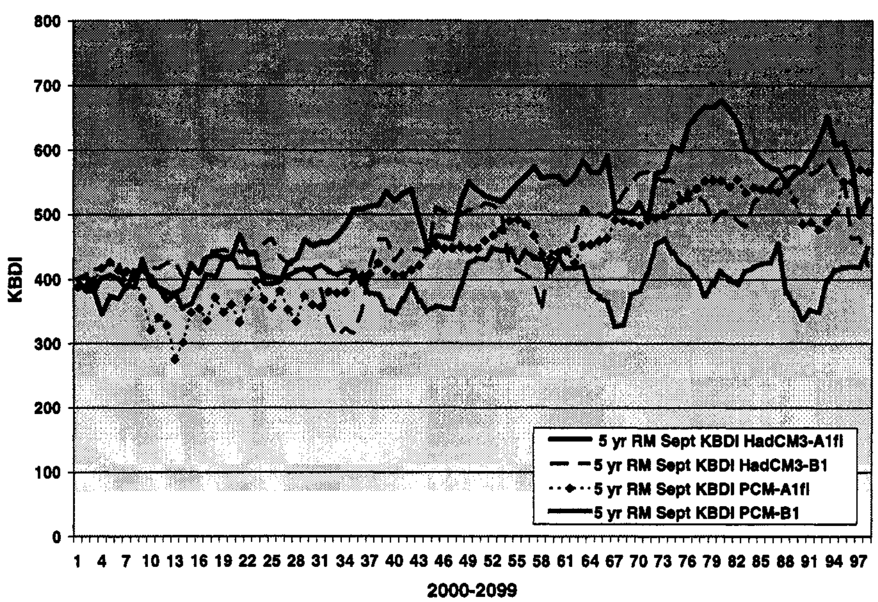

Figure 28: 5-year running mean of KBDI values for September, 2000-2099 for all the four models for Sequoia National Park (118°45′ W, 36°35′ N, elevation 2,135 m).

Summarized Results in the Form of Histograms

The results for KBDI are summarized in histograms with number of days greater than a threshold KBDI (300, 350, 400, 500, and 600). The "KBDI> threshold" includes all the days that have KBDI greater than the indicated value. For example KBDI>350 for August 1970-99 includes all the days in the month of August for 1970-99 when the KBDI is greater than 350. These histograms are plotted for the periods 1970-1999, 2020-2049, and 2070-2099 for July, August, and September.

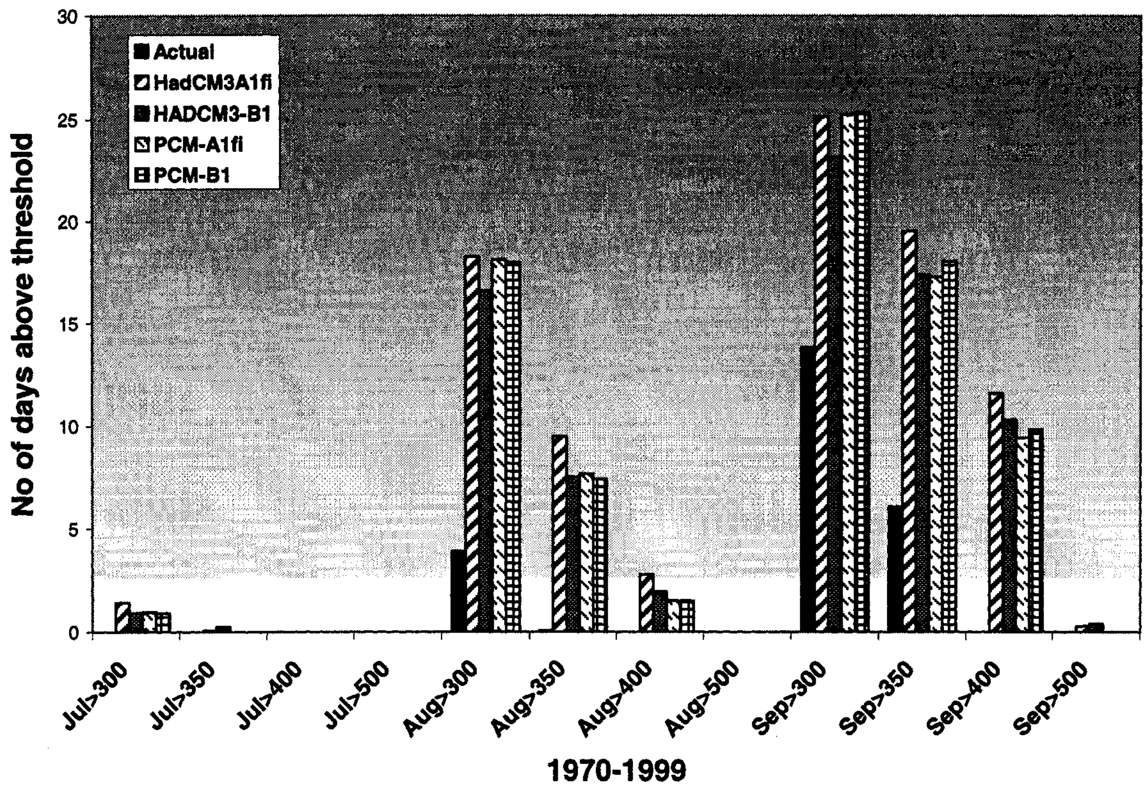

Figure 29: Number of days during 1970-1999 with the KBDI > threshold for Sequoia National Park (118^{0}45′ W, 36^{0}35′ N and elevation 2,135 m).

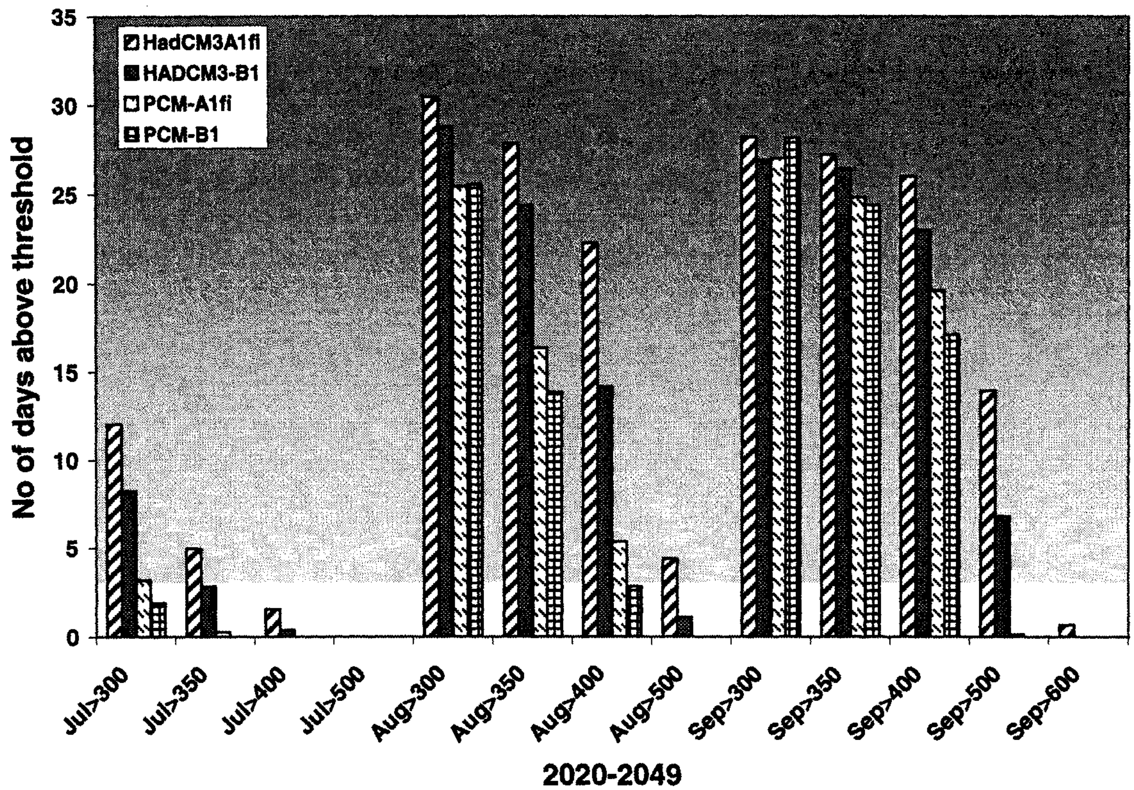

Figure 30: Number of days during 2020-2049 with the KBDI > threshold for Sequoia National Park ($118^0 45'$ W, $36^0 35'$ N and elevation 2,135 m).

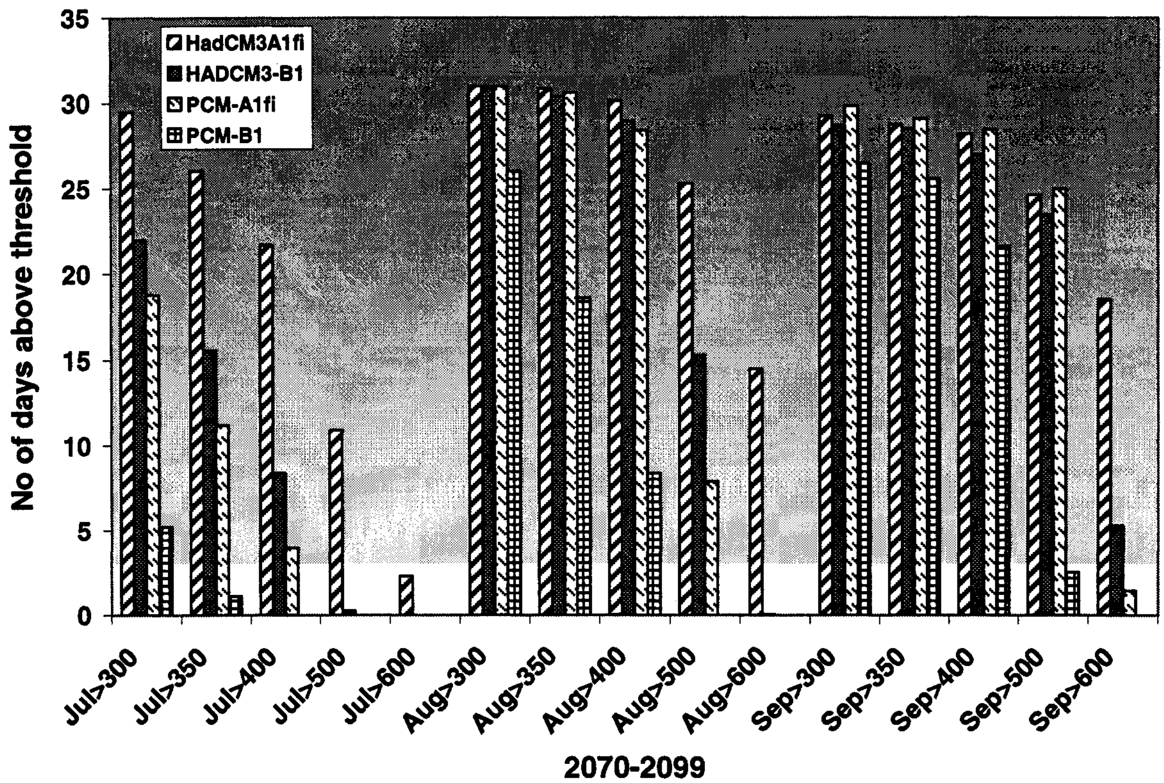

Figure 31: Number of days during 2070-2099 with the KBDI > threshold for Sequoia National Park (118^{0}45′ W, 36^{0}35′ N and elevation 2,135 m.

Figures 29-31 show the number of days during 1970-99, 2020-2049, and 2070-2099 with KBDI greater than five thresholds (300, 350, 400, 500 and 600) for the models HadCM3-A1fi, HadCM3-B1, PCM-A1fi and PCM-B1. During the baseline period 1970-1999, the actual KBDI value (calculated from the actual daily temperature and precipitation data) for the park does not cross KBDI value of 350. The models follow roughly the same emissions pathway. The slight differences between model runs during 1970-99 should be due to internal model variability.

The Figures 32-34 and Tables 5-7 also show the summer drought projection for the Sequoia National Park with yearly summer drought days (KBDI>300, 400 and 500). Comparison of the three figures for the period 1970-99, 2020-49, and 2070-99 shows that the summer drought days (Jul-Sept) increases progressively during the 21st century. Towards the end of the century, drought days with KBDI>500 are significant, as compared to 1970-99.

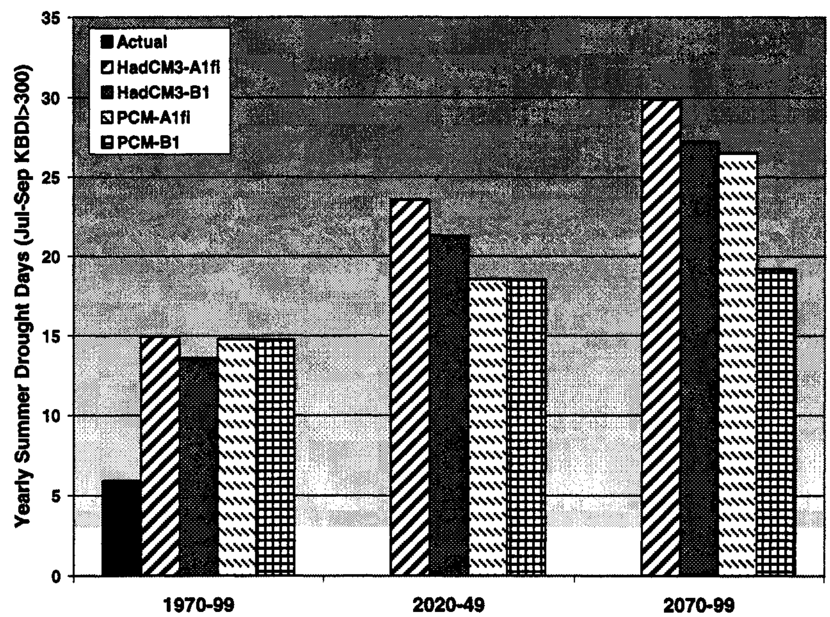

Figure 32: 21st century summer (Jul-Sept) drought projection for Sequoia National Park ($118^0 45'$ W, $36^0 35'$ N, elevation 2,135 m) showing the number of days with KBDI >300.

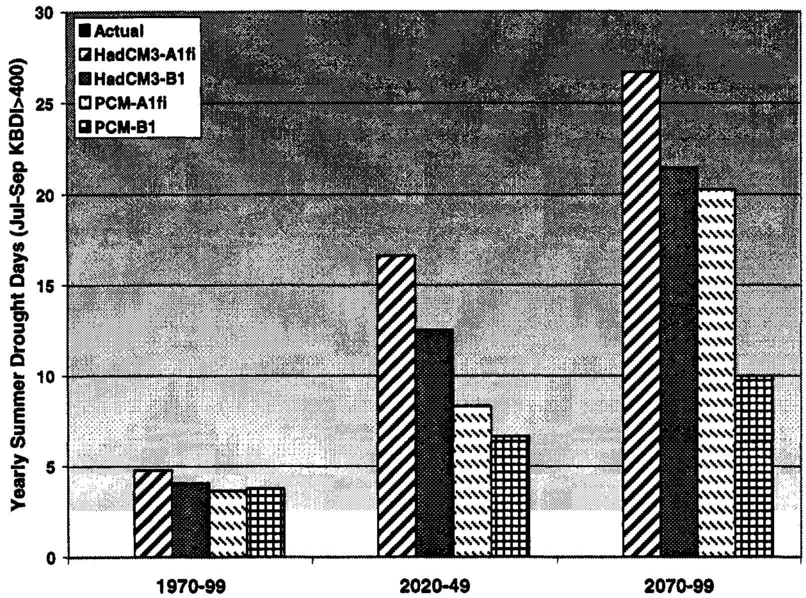

Figure 33: 21st century summer (Jul-Sept) drought projection for Sequoia National Park (118°45′ W, 36°35′ N, elevation 2,135 m) showing the number of days with KBDI >400.

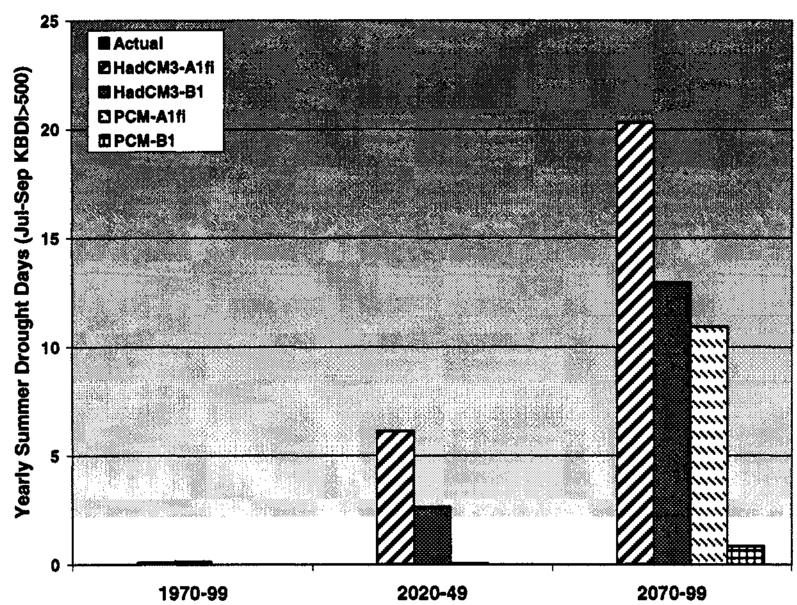

Figure 34: 21st century summer (Jul-Sept) drought projection for Sequoia National Park (118°45′ W, 36°35′ N, elevation 2,135 m) showing the number of days with KBDI >500.

Table 5: 21st century summer (Jul-Sept) drought projection for Sequoia National Park ($118^0 45'$ W, $36^0 35'$ N, elevation 2,135 m) showing the number of days with KBDI>300.

1970-99 KBDI days	**July>300**	**Aug>300**	**Sept>300**	**Total**	**Average (Total/3)**
Actual	0	3.9	13.83	17.73	5.91
HadCM3-A1fi	1.43	18.27	25.13	44.83	14.94
HadCM3-B1	0.93	16.6	23.17	40.70	13.57
PCM-A1fi	0.97	18.1	25.23	44.30	14.77
PCM-B1	0.9	17.97	25.3	44.17	14.72
2020-49 KBDI days	**July>300**	**Aug>300**	**Sept>300**	**Total**	**Average (Total/3)**
HadCM3-A1fi	12.03	30.47	28.2	70.7	23.57
HadCM3-B1	8.23	28.8	26.9	63.93	21.31
PCM-A1fi	3.2	25.43	27.03	55.66	18.55
PCM-B1	1.9	25.53	28.17	55.6	18.53
2070-99 KBDI days	**July>300**	**Aug>300**	**Sept>300**	**Total**	**Average (Total/3)**
HadCM3-A1fi	29.5	31	29.23	89.73	29.91
HadCM3-B1	21.97	31	28.7	81.67	27.22
PCM-A1fi	18.77	31	29.83	79.6	26.53
PCM-B1	5.2	26	26.47	57.67	19.22

Table 6: 21st century summer (Jul-Sept) drought projection for Sequoia National Park ($118^0 45'$ W, $36^0 35'$ N, elevation 2,135 m) showing the number of days with KBDI>400.

1970-99 KBDI days	**July>400**	**Aug>400**	**Sept>400**	**Total**	**Average (Total/3)**
Actual	0	0	0	0	0
HadCM3-A1fi	0	2.77	11.6	14.37	4.79
HadCM3-B1	0	1.97	10.3	12.27	4.09
PCM-A1fi	0	1.53	9.43	10.96	3.65
PCM-B1	0	1.53	9.83	11.36	3.79
2020-49 KBDI days	**July>400**	**Aug>400**	**Sept>400**	**Total**	**Average (Total/3)**
HadCM3-A1fi	1.57	22.3	26	49.87	16.62
HadCM3-B1	0.37	14.17	23	37.54	12.51
PCM-A1fi	0	5.37	19.63	25	8.33
PCM-B1	0	2.83	17.13	19.96	6.65
2070-99 KBDI days	**July>400**	**Aug>400**	**Sept>400**	**Total**	**Average (Total/3)**
HadCM3-A1fi	21.7	30.13	28.2	80.03	26.68
HadCM3-B1	8.4	28.97	26.97	64.34	21.45
PCM-A1fi	3.97	28.4	28.47	60.84	20.28
PCM-B1	0	8.37	21.63	30	10.00

Table 7: 21st century summer (Jul-Sept) drought projection for Sequoia National Park ($118^0 45'$ W, $36^0 35'$ N, elevation 2,135 m) showing the number of days with KBDI >500.

1970-99 KBDI days	**July>500**	**Aug>500**	**Sept>500**	**Total**	**Average (Total/3)**
Actual	0	0	0	0	0
HadCM3-A1fi	0	0	0.27	0.27	0.09
HadCM3-B1	0	0	0.4	0.4	0.13
PCM-A1fi	0	0	0	0	0
PCM-B1	0	0	0	0	0
2020-49 KBDI days	**July>500**	**Aug>500**	**Sept>500**	**Total**	**Average (Total/3)**
HadCM3-A1fi	0	4.4	13.93	18.33	6.11
HadCM3-B1	0	1.1	6.8	7.9	2.63
PCM-A1fi	0	0	0.13	0.13	0.04
PCM-B1	0	0	0	0	0.00
2070-99 KBDI days	**July>500**	**Aug>500**	**Sept>500**	**Total**	**Average (Total/3)**
HadCM3-A1fi	10.9	25.3	24.63	60.83	20.28
HadCM3-B1	0.23	15.27	23.47	38.97	12.99
PCM-A1fi	0	7.87	24.97	32.84	10.95
PCM-B1	0	0	2.53	2.53	0.84

Comparison of Actual KBDI and Model Simulated KBDI Days for 1970-99

Figures 29 and 32 show that there is a considerable difference in the number of KBDI days>threshold (300 and 350) for the actual data and model simulated data for the months of August and September, 1970-99. This can be explained with the help of the table 8 below, which shows a comparison of the actual KBDI data for the park (computed using actual daily temperature and precipitation data) and KBDI data computed from the model simulated daily temperature and precipitation data.

Table 8: Comparison of actual and simulated KBDI days for Sequoia National Park ($118^0 45'$ W, $36^0 35'$ N, elevation 2,135 m).

KBDI DATA 1970-1999	Aug>300 KBDI days	Aug>350 KBDI days	Sept>300 KBDI days	Sept>350 KBDI days
Actual	3.9	0.07	13.83	6.07
HadCM3-A1fi	18.27	9.5	25.13	19.53
HadCM3-B1	16.6	7.53	23.17	17.37
PCM-A1fi	18.1	7.67	25.23	17.27
PCM-B1	17.97	7.4	25.3	18.03

Table 8 shows that for the period (1970-99), the actual number of days with KBDI >300 and 350 (for August and September) for the park are far less than the model simulated KBDI days. The reason for this is that the actual temperature (Tmax) for the park is lower than the model simulated temperature as shown in the Figure 35. Similarly, the actual precipitation for the park is higher than the model simulated precipitation as shown in the Figure 36. Lower temperature and higher precipitation result in lower KBDI values.

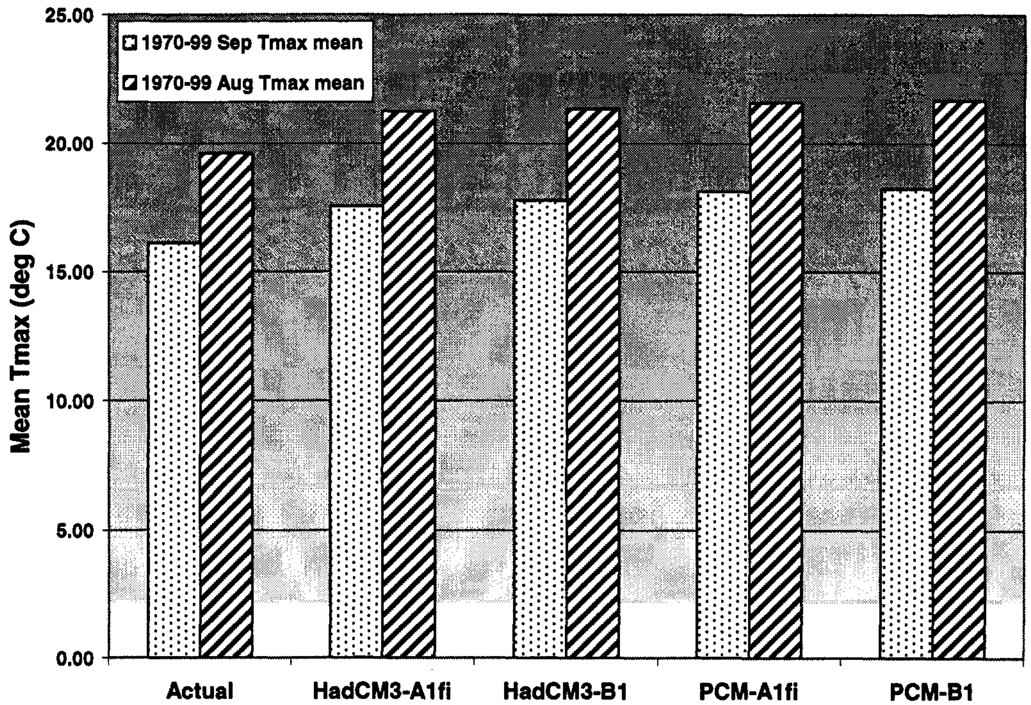

Figure 35: Mean August and September temperature (T max) for Sequoia National Park ($118^0 45'$ W, $36^0 35'$ N, elevation 2,135 m) for actual and model simulated temperature data (1970-1999).

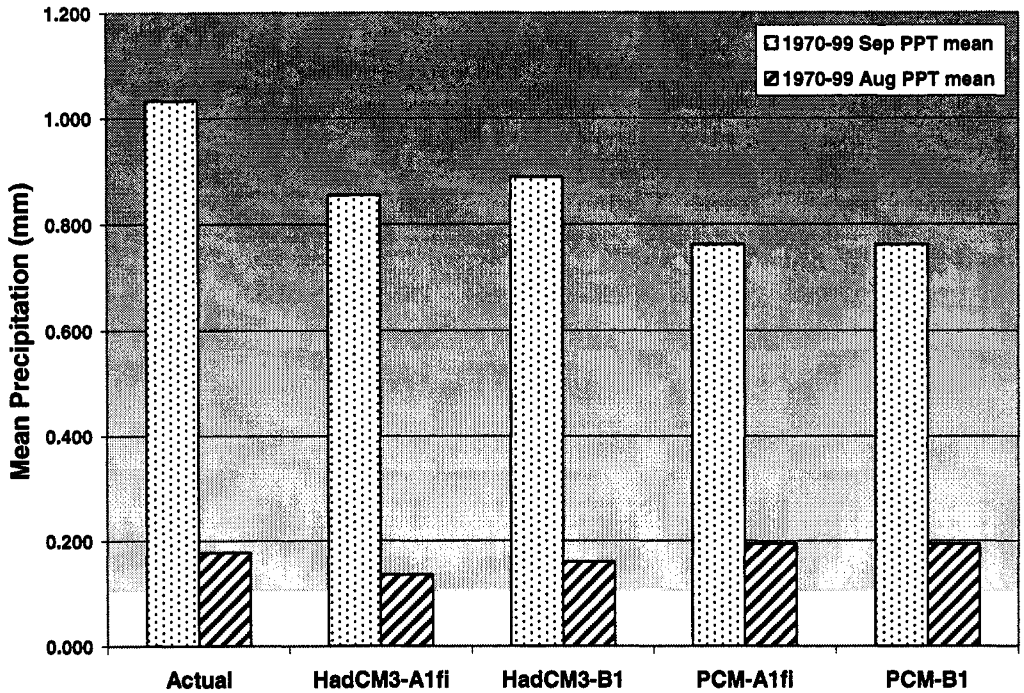

Figure 36: Mean August and September precipitation for Sequoia National Park ($118^0 45'$ W, $36^0 35'$ N, elevation 2,135 m) for actual and model simulated precipitation data (1970-1999).

Table 9 shows the KBDI days>threshold during 2020-2049 for all the models. During this period, KBDI values greater than 500 start making appearance, indicating severe drought conditions.

Table 9: Comparison of KBDI days > threshold for the period 2020-2049 for Sequoia National Park (118^{0}45′ W, 36^{0}35′ N, elevation 2,135 m).

Models 2020-49	Aug KBDI>400	Aug KBDI>500	Sept KBDI>400	Sept KBDI>500
HadCM3-A1fi	22	4	26	14
HadCM3-B1	14	1	23	7
PCM-A1fi	5	0	20	0
PCM-B1	3	0	17	0

HadCM3-A1fi shows the higher number of days and PCM-B1 shows the lowest number of days with KBDI>400 and 500. Also, the number of days with KBDI> threshold increases from Aug-Sept. 2070-2099 has a significant increase in the number of days with KBDI> 400, 500, and 600. Table 10 shows the KBDI days >threshold during 2070-2099 for all the models.

Table 10: Comparison of KBDI days >threshold for the period 2070-2099 for Sequoia National Park (118^{0}45′ W, 36^{0}35′ N, elevation 2,135 m).

Models 2070-99	Aug KBDI>400	Aug KBDI>500	Aug KBDI>600	Sept KBDI>400	Sept KBDI>500	Sept KBDI>600
HadCM3-A1fi	30	25	15	28	25	19
HadCM3-B1	29	15	0	27	23	5
PCM-A1fi	28	8	0	28	25	1
PCM-B1	8	0	0	22	3	0

During September 2070-2099 there is not much difference between the KBDI days>400 and 500 for HadCM3-A1fi, HadCM3-B1, and PCM-A1fi, despite the fact that PCM is a low sensitivity model as compared to HadCM3. This anomaly can be explained by the following Figures 37 and 38.

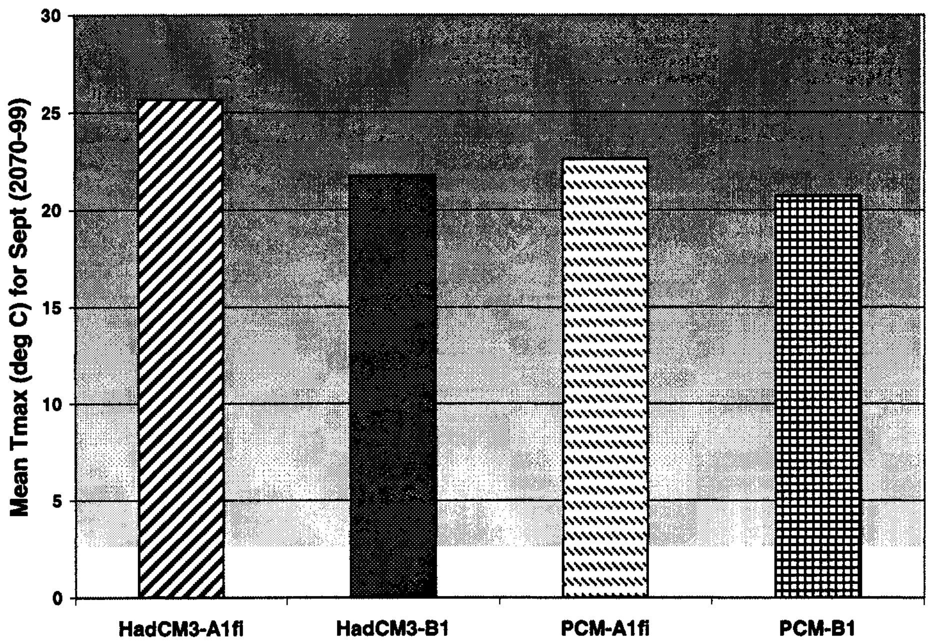

Figure 37: Mean September temperature for 2070-99 for Sequoia National Park (118^{0}45′ W, 36^{0}35′ N, elevation 2,135 m).

Figure 37 shows that the mean temperature for September 2070-99 for HadCM3-A1fi is 26^{0}C, HadCM3-B1 is 22^{0}C, PCM-A1fi is 23^{0}C, and PCM-B1 is 21^{0}C. The high mean temperature for September during 2070-99 for PCM-A1fi may be the reason for higher number of days with KBDI> 400 and 500 (KBDI value increases with the increase in temperature). Also there is not much difference between the mean temperatures for

PCM-A1fi (23^{0}C) and HadCM3-B1 (22^{0}C), even though A1fi is a high scenario and B1 is a low emission scenario. This may explain PCM-A1fi having more or less similar KBDI days> threshold to HadCM3-B1.

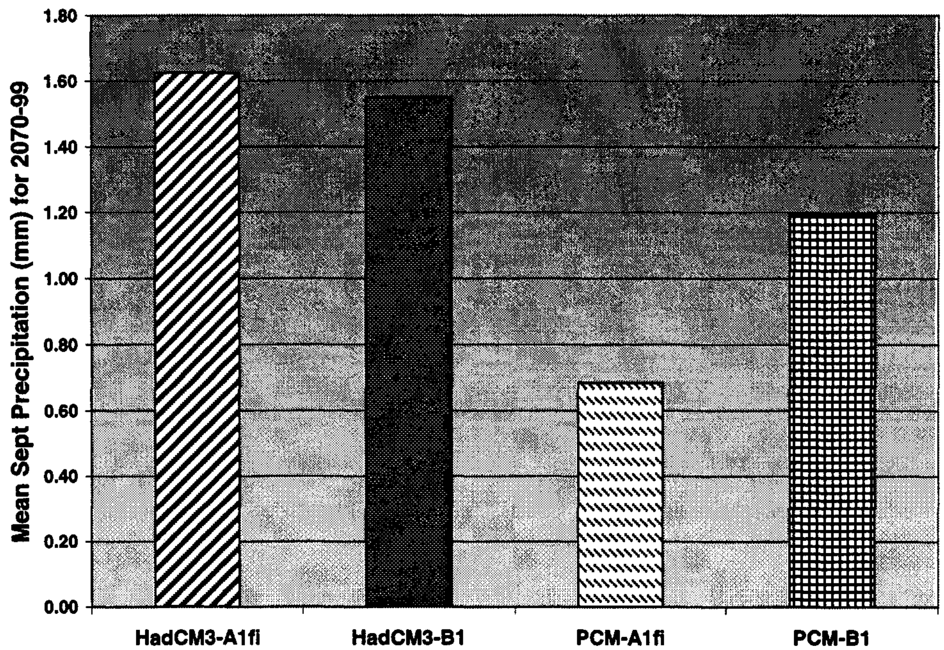

Figure 38: Mean September precipitation (in) for 2070-99 for Sequoia National Park (118^{0}45′ W, 36^{0}35′ N, elevation 2,135 m).

Similarly, Figure 38 shows the September mean precipitation for HadCM3-A1fi is 1.58 mm, for HadCM3-B1 it is 1.55 mm, for PCM-A1fi it is 0.69 mm, and for PCM-B1 it is 1.19. This lower mean precipitation during September 2070-99 for PCM-A1fi may be the reason for the higher number of days with KBDI> 400 and 500 as compared to HadCM3-B1.

Sensitivity Analysis of the Models

Table 11 shows the comparison of the actual temperature and model simulated temperature (mean Tmax) and mean precipitation data for 1970-99.

<u>Table 11</u>: Comparison of the actual temperature and model simulated temperature data for 1970-99, along with the detrended standard deviation*.

AUG AND SEPT MEAN TEMPERATURE (Tmax in deg C) FOR 1970-1999					
STATS	Actual	HadCM3-A1fi	HadCM3-B1	PCM-A1fi	PCM-B1
Aug Mean Tmax (deg C)	20	21	21	22	22
Std Dev after detrending	1.4	1.3	1.4	1.2	1.3
Sept Mean Tmax	16	18	18	18	18
Std Dev after detrending	2.0	1.4	1.3	1.4	1.4
AUG AND SEPT MEAN PRECIPITATION (mm) FOR 1970-1999					
Aug Mean PPT	0.1	0.1	0.3	0.2	0.2
Std Dev after detrending	0.3	0.2	0.4	0.2	0.2
Sept Mean PPT	1.0	0.8	0.9	0.8	0.8
Std Dev after detrending	1.6	1.0	1.0	1.0	0.8

*<u>Detrended Standard Deviation</u>: When trends are observed in data points, the trend can be removed by rotating the data around the mean. This often "spreads out" the data, thereby allowing the user to detect patterns of deviations more easily.

The detrended standard deviation for the actual mean temperature (Tmax in degrees C) and precipitation (mm) is higher than the models, for August and September, though only significantly so for September mean Tmax. All the models have more or less the same detrended standard deviation, and lower than the actual. It is important that the difference between model computed KBDI and the actual KBDI be kept in mind when interpreting the model calculated KBDI. First, the model temperatures are higher, which causes higher KBDI. Second the models variance is lower, for which it is hard to say what effect it causes, if any. The above analysis shows that the KBDI values calculated for the 21st century using the model projected temperature and precipitation are good for indicating possible relative changes in frequency of high KBDI values.

PCM-B1 does not show considerably higher KBDI days when compared to HadCM3-A1fi, HadCM3-B1, and PCM-A1fi. This is because PCM-B1 projects a slight increase in precipitation ($\approx$ 7%) by the end of the century and may be a wet model (Hayhoe et al, 2004). Higher precipitation results in lower KBDI. The KBDI days>400 and 500 for HadCM3-A1fi and PCM-A1fi are very comparable during 2070-2099. This is in spite the fact the PCM is a low sensitivity model as compared to HadCM3. The results essentially indicate that the emission pathways we follow are likely to determine the future wildfire risk experienced in the study region.

CONCLUSIONS

The Intergovernmental Panel on Climate Change (IPCC) has concluded that the climate has changed over the past century, human activities are responsible for influencing these changes, and that climate is expected to continue to change in the future. Depending on the emission scenarios assumed, continued increases in concentrations of greenhouse gases in the atmosphere are expected to induce and additional 1.4^0C to 5.8^0C increase in average global temperatures by the year 2100. It is also certain that precipitation will change, bringing the threat of extreme droughts to some regions while others may experience fewer droughts or even flooding. The response of forests to an increase in drought conditions is considered a key issue in climate change scenario. Changes in drought conditions are likely to affect the extent of wildfire risk potential, with ramification for many forests where natural fire regimes have been suppressed by forest management activities, leading to the build up of readily available forest fuel and increasing the risk of wildfire. How the forests are drying as a result of drought, changing temperatures and precipitation, and how the wildfire risk potential is likely to change over the 21^{st} century has been studied through the climatic indicator, Keetch and Byram's Drought Index (KBDI).

Because the drought index is based on the water availability for transpiration, the index is on a scale ranging from 0-800. However, the association of KBDI values with fire risk or intensity must be done location by location (Keetch and Byram, 1968). The results show that as the KBDI goes up, the wildfire risk potential for the park increases, in terms of more severe fires. The purpose of the drought index is to provide forest management personnel with a scale of reference for estimating the conditions in the area. This information can be used in planning fire control operations. The study shows that for the month of August and September, the number of days with KBDI> 400, 500 and 600 increases towards the end of the century for all the models, particularly HadCM3-A1fi, HadCM3-B1, and PCM-A1fi. The KBDI values calculated for the 21^{st} century using the model projected temperature and precipitation indicate that there is a potential increase drought conditions during the 21^{st} century, as everything above 400 (KBDI) is considered severe drought. And this implies that the wildfire risk for the park increases considerably.

It would be useful for future work to attempt to factor in vegetation change resulting from climate change. Because inter-decadal variability often dominates precipitation over California, projected changes in climate and impacts associated with the effects of precipitation are subject to uncertainty. Shifts in seasonal characteristics, annual cycles, and geographical gradients of precipitation can strongly affect soil moisture, and this is an important variable in the development of drought conditions.

The results support the idea that climate change and many of its impacts scale with the quantity and timing of greenhouse gas emissions. It represents a solid starting point for assessing the outcome of changes in greenhouse gas emission trajectories driven by climate-specific policies and the extent to which lower emissions can reduce the likelihood and thus risks of ''dangerous anthropogenic interference with the climate system'' (United Nations, 1992).

FUTURE RESEARCH NEEDS

This study estimated the drought conditions and the fire risk potential for the 21st century assuming that no change in the vegetation takes place. A vegetation model can be applied to the above studied scenarios to study how the vegetation might change in the 21st century, and how this change in forest structure and composition further affects the fire risk. It will also be useful to compare the conclusions drawn here using KBDI with those using other drought indexes like the Palmer Drought Severity Index (PDSI) or other forest fire indicators like the Energy Release Component (ERC).

Better management strategies can be proposed based on these results. Fire personnel should be alert for KBDI levels that depart from the normal yearly patterns, especially during summer fire season. From a forest fire perspective, it is essential to observe the impact of climate change regularly, not just when a drought appears to be looming. This is essential information source that helps drive fire preparedness, staffing level, and assists in synchronizing resource management strategies, including seasonal firefighters, equipment and aircraft availability. It will also be useful to study how El Nino-Southern Oscillation (ENSO) will modulate fire activity in the 21st century.

REFERENCES

Andrews, P.L., and Bradshaw, L.S. 1996. Interpretation of the National Fire Danger Rating System for Yellowstone National Park. Ecological Implication of fire in Greater Yellowstone, ICWF: 211-216.

Bradshaw, L. S., Deeming, J. E., Burgan, R. E., Cohen, J. D. 1984. The 1978 National Fire-Danger Rating System; technical documentation. *General Technical Report INT-169.* Ogden, UT: U.S.D.A, Forest Service, Intermountain Forest and Range Experiment Station: 44pp.

Brown, T.J., Hall, B.L., and Westerling, A.L. 2004. The Impact of Twenty-first Century Climate Change on Wildland Fire Danger in the Western United States: An Applications Perspective. *Climatic Change* 62: 365-388.

Brown, P.M., and Swetnam, T.W. 1994. A cross-dated fire history from a stand of coast redwood near Redwood National Park, California. *Canadian Journal of Forest Research* 24: 21-31.

Burgan, R. E. 1988. Revisions to the 1978 National Fire-Danger Rating System. *Res. Pap. SE-273.* Asheville, NC: U.S.D.A, Forest, Service, Southeastern Forest Experiment Station: 39pp.

California Board of Forestry. 1996. California fire plan - a framework for minimizing costs and losses from wildland fires. Sacramento, CA.

Fischer, G., Shah, M., and Velthuizen, H. 2002. Climate Change and Agricultural Vulnerability. International Institute for Applied Systems Analysis. Report prepared under UN Institutional Contract Agreement 1113 for World Summit on Sustainable Development. Laxenburg, Austria.

Flannigan, M. D., Stocks, B.J., and Wotton, B.N. 2000. Climate change and forest fires. *The Science of the Total Environment* 262: 221-229.

Flannihan, M.D., and Wagner, V. 1990. Climate change and wildfire in Canada. *Can. J. Forest Res* 21: 66-72.

Fried, J.S., Torn, M.S., Mills, E. 2004. The impact of climate change on wildfire severity: A regional forecast for northern California. *Climatic Change* 64: 169-191.

Fujioka, F. M. 1991. Starting up the Keetch-Byram Drought Index. Extended Abstract, 11th Conf. on Fire and Forest Meteor., Missoula Montana: 74-80.

Gordon, C.C., Cooper, C.A., Senior, H. B., Gregory, J.M., Johns, T.C., Mitchell, J.F.B., and Wood, R.A. 2000. The simulation of SST, sea ice extents and ocean heat transports in a version of the Hadley Centre coupled model without flux adjustments. *Climate Dynamics* 16: 147-168.

Graumlich, L. J. 1993. A 1000-year record of temperature and precipitation in the Sierra-Nevada. *Quaternary Research* 39:249–55.

Groisman, P.Y., Knight, R.W., Heim, R.R., Razuvaev V.N., Sherstyukov, B.G., Speranskaya, N.A. 2003. Contemporary climate changes in high latitudes of the Northern Hemisphere cause an increasing potential forest fire danger. *5th Symposium on Fire and Forest Meteorology*: 1-6.

Hayhoe, K., Cayan, D., Field, C.B., Frumhoff, P.C., Maurer, E.P., Miller, N.L., Moser, S.C., Schneider, S.H., Cahill, K.N., Cleland, E.E., Dale, L., Drapek, R., Hanemann, R.M., Kalkstein, L.S., Lenihan, J., Lunch, C.K., Neilson, R.P., Sheridan, S.C., and Verville, J.H. 2004. Emissions pathways, climate change, and impacts on California: *PNAS* 101: 12422-12427.

Houghton, J. 2005. Global warming. *Rep. Prog. Phys.* 68:1343–1403.

Kattelmann, R. 1996. Hydrology and water resources. *In*: Status of the Sierra Nevada. Vol. II. Assessments and scientific Basis for Management Options. *Wildland Resources Center Report No. 37.* University of California, Davis.

Keetch, J.J., and Byram, G.M. 1968. A drought index for forest fire control. *U.S.D.A. Forest Service Research Paper SE-38*: 35 pp.

Lenihan, J.M., Drapek, R.J., Bachelet, D., and Neilson, R.P. 2003. Climate change effects on vegetation distribution, carbon, and fire in California. *Ecological Applications* 13(6):1667-1681.

Lenihan, J.M., Drapek, R.J., Bachelet, D., and Neilson, R.P. 2004. Western forests, fire risk, and climate change. Pacific Northwest Research Station 6.

McKelvey, K.S., and Busse, K.K. 1996. Twentieth-century fire patterns on forest service lands. 1996. Sierra Nevada Ecosystem Project: Final report to Congress, Vol II, Assessments and scientific basis for management options. Centers of Water and Wildland Resources. University of Davis, Davis.

Mckenzie, D., Gedalof, Z., Peterson, D.L., Mote, P. 2004. Climatic change, wildfire, and conservation. *Conservation Biology* 18: 890-902.

McMichael, A.J., Haines, A., and Slooff, R. 1996. Climate Change and Human Health. World Health Organization, World Meteorological Organization, United Nations Environmental Program, Geneva: 305.

Melton, M. 1989. The Keetch-Byram Drought Index: A guide to fire conditions and suppression problems. Fire Management Notes: HO2-IIIA-NFDRS, Vol 50, no 4.

Miller, C., and Urban, D.L. 1999. Forest pattern, fire, and climatic change in the Sierra Nevada. *Ecosystems* 2:76-87.

Nakic´enovic´, N., Alcamo, J., Davis, G., de Vries, B., Fenhann, J., Gaffin, S., Gregory, K., Gru¨bler, A., Jung, T. Y., Kram, T., et al. 2000. *Intergovernmental Panel on Climate Change Special Report on Emissions Scenarios* (Cambridge Univ. Press, Cambridge, U.K.

Overpeck, J.T., Rind, D., and Goldberg, R. 1990. Climate induced changes in forest disturbances and vegetation. *Nature* 343: 51-53.

Stephens, S.L., Skinner, C.N., Gill, S.J. 2003. Dendrochronology- based fire history of Jeffrey pine-mixed conifer forests in the Sierra San Pedro Martir, Mexico. *Canadian Journal of Forest Research*. 33: 1090-1101.

Stephenson, N.L. 1988. Climatic control of vegetation distribution: role of the water balance with examples from North America and Sequoia National Park, California. *Ph.D. dissertation*. Cornell University, Ithaca.

Pope, V.D., Gallani, M.L., Rowntree, P.R., and Stratton, R.A. 2000. The impact of new physical parametrizations in the Hadley Centre climate model -- HadAM3. *Climate Dynamics*, 16: 123-146.

Preisler, K.H., and Weise, R.D. Forest fire models. Pacific Southwest Research Station, U.S.D.A, Forest service.

Pyne, S.J., Andrews, P. L., and Laven, R.D. 1996. Introduction to Wildland fire. New York: John Wiley & Sons, Inc.

Rind, D.R., Hansen, G.J., Rosenzweig, C., and Ruedy, R. 1990. Potential evapotranspitation and the likelihood of future drought. *J. Geophy. Res.* 95: 9983-10004.

Sapsis, D., Bahro, B., Gabriel, J., Jones, R., and Greenwood, G. 1996. An assessment of current risks, fuels, and potential fire behavior in the Sierra Nevada. *In*: Status of the Sierra Nevada. Vol. III. Assessments and scientific Basis for Management Options. *Wildland Resources Center Report No. 37*. University of California, Davis.

Schneider, S.H. 1989. The greenhouse effect: science and policy. *Science* 243: 771-781.

Stocks, B.J., Fosberg, M.A., Lynham, T.J., Mearns, L., Wotton, B.M., Yang, Q., Jin, J-Z., Lawrence, K.M., Hartley, G.R., Mason, J.A., and McKenney, D.W. 1998. Climate change and forest fire potential in Russian and Canadian boreal forests. *Climatic Change* 38: 1-13.

Swetnam, T. W. 1993. Fire history and climate change in giant sequoia groves. *Science* 262:885-889.

Swetnam, T.W., and Baisan, C.H. 2003. Tree-ring reconstructions of fire and climate history in the Sierra Nevada and southwestern United States. Pages 158-195 in Veblen, T.T., Baker, W.L., Montenegro, G., and Swetnam, T.W. 2003. Fire and climate change in temperate ecosystems of the western Americas. *Ecological Studies 160*. New York: Springer-Verlag, Inc.

Torn, M.S., and Fried, J.S. 1992. Predicting the impacts of global warming on wildland fire. *Climate Change* 21: 257-274.

Torn, M.S., Mills, E., and Fried. J. 1998. Will climate change spark more wildfire damage? *Lawrence Berkeley National Laboratory Report No. 42592.*

Torn, M.S., Mills, E., and Fried. J. 2004. The impact of climate change in wildfire severity: A regional forecast for Northern California. *Climate Change* 64: 169-191.

United Nations. 1992. United Nations Framework Convention on Climate Change (United Nations, Rio de Janeiro, Brazil).

Veblen, T.T., Baker, W.L., Montenegro, G., and Swetnam, T.W. 2003. Fire and climate change in temperate ecosystems of the western Americas. *Ecological Studies 160*. New York: Springer-Verlag, Inc.

Weber, M.G., and Flannigan, M.D. 1997. Canadian boreal forest ecosystem structure and function in a changing climate: Impact on fire regimes. *Environ. Rev 5*: 145-166.

Weatherspoon, C.P. 1996. Fire-silviculture relationships in Sierra forests. *In*: Status of the Sierra Nevada. Vol. II. Assessments and scientific Basis for Management Options. *Wildland Resources Center Report No. 37*. University of California, Davis.

Wigley, T.M., Briffa, K.R., and Jones, P.D. 1984. Predicting plant productivity and water resources. *Nature* 312: 102-103.

Wilkinson, C.O., Linden, H.C., Hodgson, G., Rubens, J., and Strong, A.E. 1999. Ecological and socioeconomic impacts of 1998 coral mortality in the Indian Ocean: An ENSO impact and a warning of future change? *Ambio* 28: 188-196.

Wotton, B.M., Martell, D.L., and Logan, K.A. 2003. Climate change and people-caused forest fire occurrence in Ontario. *Climatic Change* 60: 275-295.

APPENDIX A

Map of Sequoia and Kings Canyon National Park

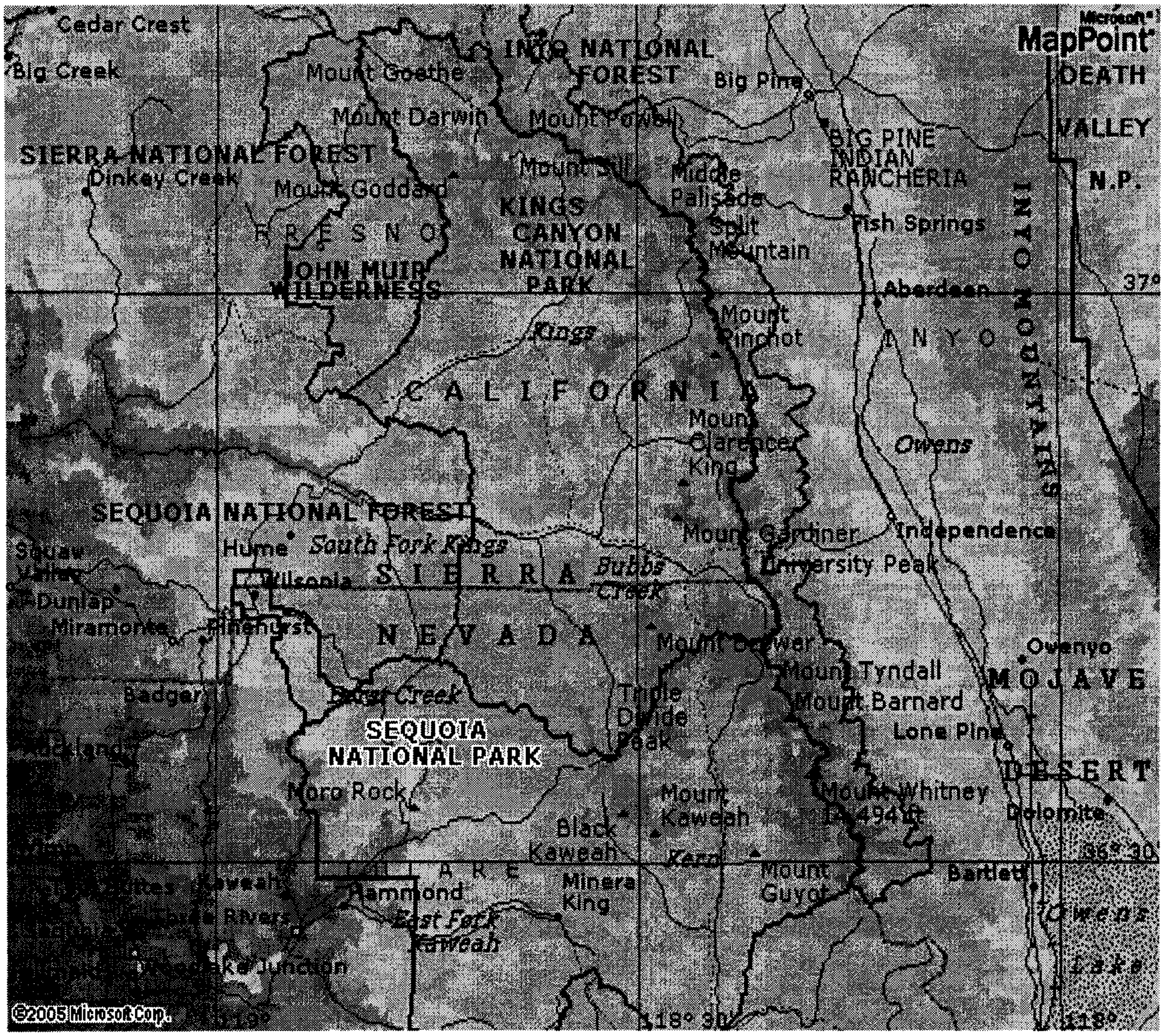

Source of map: http://encarta.msn.com

APPENDIX B

Flowchart for KBDI Calculations

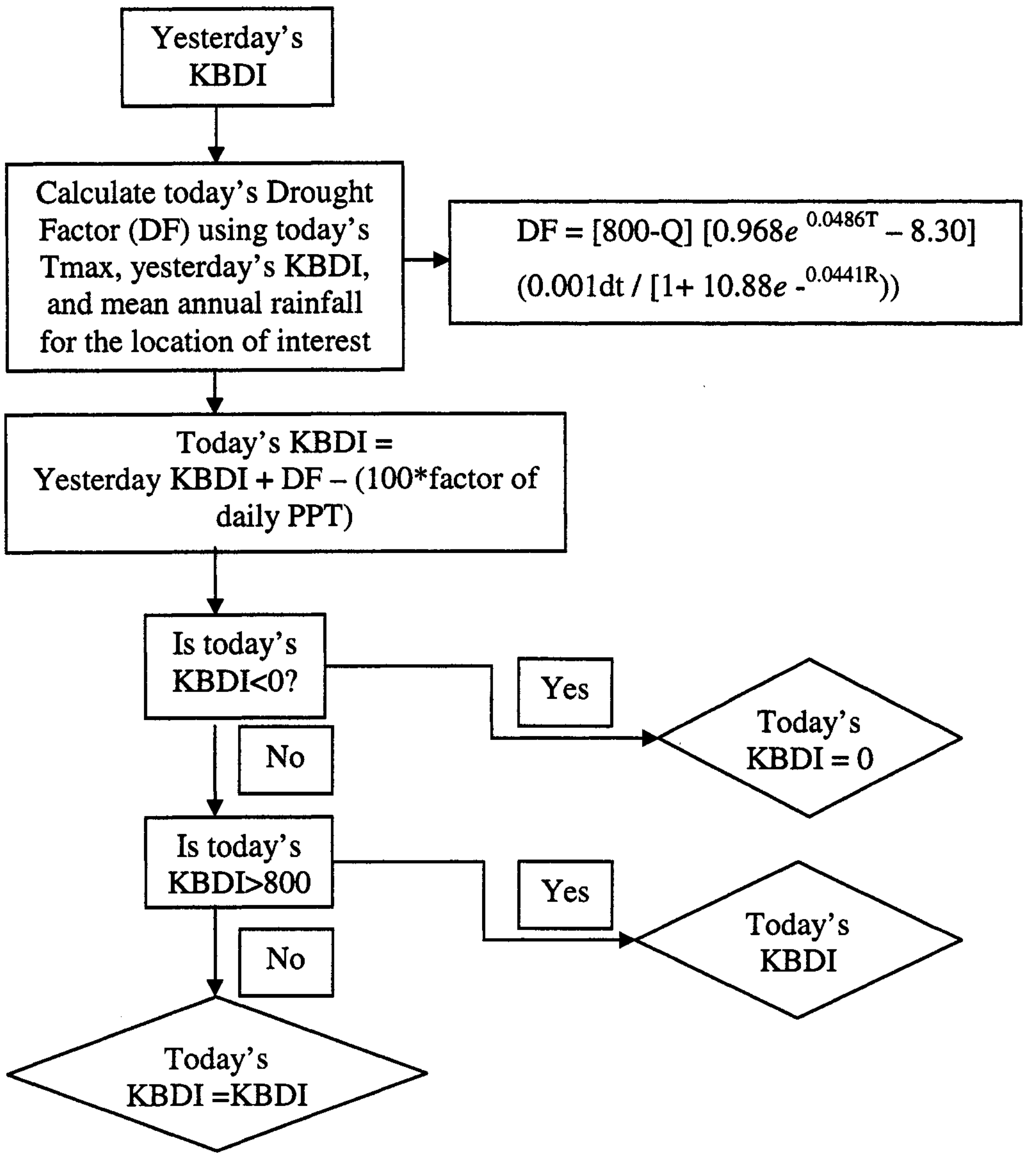

APPENDIX C

Fire Term Glossary

Available Fuel - Is the portion of the total fuel that actually burns.

Drought Index – Is the number representing net effect of evaporation, transpiration and precipitation in producing cumulative moisture depletion in deep duff or upper soil layers.

Duff - The partially decomposed organic material of the forest floor beneath the litter or freshly fallen twigs, needles and leaves.

El Niño - A major warming of the equatorial waters in the Pacific Ocean. El Nino events usually occur every 3 to 7 years, and are characterized by shifts in "normal" weather patterns

ENSO - A complex interaction of the tropical Pacific Ocean and the global atmosphere that results in irregularly occurring episodes of changed ocean and weather patterns in many parts of the world, often with significant impacts, such as altered marine habitats, rainfall changes, floods, droughts and changes in storm patterns

Fire Danger Rating - A fire management system that integrates the effects of selected fire danger factors into one or more qualitative or numerical indices of current protection needs.

Fire Frequency - The return interval or recurrence interval of fire in a given area over a specific time

Fire Intensity - The rate of heat release for an entire fire at a specific point in time.

Fire Regime - The characteristics of fire in a given ecosystem, such as the frequency, predictability, intensity, and seasonality of fire.

Fire Severity - Degree to which a site has been altered or disrupted by fire; also used to describe the product of fire intensity and residence time (McPherson and others 1990, Agee 1994, Rowe 1983).

Fuel- Fuel is comprised of living and dead vegetation that can be ignited. It is often classified as dead or alive and as natural fuels or activity fuels (resulting from human actions, usually from logging operations). Fuel components refer to such items as downed dead woody material by various size classes, litter, duff, herbaceous vegetation, live foliage etc. (Brown 2000).

Fuel Loading - The weight of fuels in a given area, usually expressed in tons per acre. Fuel loading may be referenced to fuel size or time lag categories; and may include surface fuels or total fuels.

Fuel Moisture – Percent or fraction of oven dry weight of fuel. It is the most important fuel property controlling flammability. In living plants it is physiologically bound. Its daily fluctuations vary considerably by species but are usually above 80 to 100%. As plants mature, moisture content decreases. When herbaceous plants cure, their moisture content responds as dead fuel moisture content, which fluctuates according to changes in temperature, humidity, and precipitation (Brown 2000).

Greenhouse Effect - The warming of the atmosphere by the trapping of long wave radiation being radiated to space. The gases most responsible for this effect are water vapor and carbon dioxide

Keetch-Byram Drought Index (KBDI) - A number between 0-800 representing the amount of moisture in the top 8 inches of soil. Zero is saturated, 800 is maximum drought stress. It is calculated from recent precipitation measurements in relation to the average annual precipitation. It is important to note that the KBDI is customized for each geographic area and that often the scale shows less of a range in variation.

Litter - Dead material on the ground that is little altered by decomposition. It includes freshly fallen leaves, needles, fine twigs, bark flakes, fruits, matted dead grass, and miscellaneous vegetative parts.

NFDRS (National Fire Danger Rating System) - A multiple index system developed to provide information about current and predicted fire danger conditions.

Relative Humidity (RH) - The ratio of the amount of moisture in a given volume of atmosphere to the amount that volume would contain if it were saturated. It is the ratio of the actual vapor pressure to the saturated vapor pressure.

Surface Fuels - All materials lying on, or immediately above, the ground, including needles or leaves, duff, grass, small dead wood, downed logs, stumps, large limbs, low brush and reproduction.

Vegetation Type - A standardized description of the vegetation in which a fire is burning. The type is based on the dominant plant species and the age of the forest and indicates how moist a site may be and how much fuel is likely to be present

Wildland Fire - Any non-structural Fire, other than prescribed fire that occurs in the wildland.